

PHOOTONICS

A Cost-Effective Photonics-based Device for Early Prediction, Monitoring and Management of Diabetic Foot Ulcers

Deliverable	D3.2 – Meta-analysis Results
Work Package(s)	WP3 - Medical Meta-Analysis, User Requirements and Technical Specifications
Task(s)	T3.1 - Medical Meta-Analysis on Diabetic Foot
Dissemination Level	PU
Due Date	20-04-2020
Actual Submission Date	31-07-2020
WP Leader	CHARITE
Task Leader	CHARITE
Deliverable Leader	NKUA
Contact Person	Panagiotis Terzopoulos
Phone	+37052610264
Email	panos@metisbaltic.com

Document History			
Revision	Date	Author(s)	Description
v0.1	5/3/2020	Aikaterini Angeli Doulami Andreas Lazaris	Document initialization, structure and work allocation
v0.2	7/5/2020	Aikaterini Angeli Doulami Andreas Lazaris	Advanced draft, addition of clinical features
v0.3	8/6/2020	Aikaterini Angeli Doulami Andreas Lazaris	Advanced draft
v0.4	11/6/2020	Adriane Napp	Advanced draft
v0.5	12/6/2020	Eftychios Protopapadakis Maria Kaselimi	Editing, advanced draft
v0.6	9/7/2020	Adriane Napp Günther Silbernagel Ulf Landmesser	Advanced draft
v1.0	28-07-2020	Adriane Napp Günther Silbernagel Ulf Landmesser	Editing, Final Review



PHOTONICS PUBLIC PRIVATE PARTNERSHIP

This project is an initiative of the Photonics Public Private Partnership. It has received funding from the European Union's Horizon 2020 research and innovation programme under grant agreement No 871908

This document and the information contained within may not be copied, used or disclosed, entirely or partially, outside of the PHOOTONICS consortium without prior permission of the project partners in written form

Contents

1	Introduction.....	7
2	Diabetic Ulcers: Epidemiology	9
2.1	Distribution over European Populations	9
2.2	Demographics	9
2.3	Associated Risks Factors	11
2.4	Current diagnostic/treatment cost and management	13
2.5	The Impact of early diagnosis and follow up in efficient diabetic ulcer management.....	13
3	Diabetic Ulcer pathophysiology.....	15
3.1	Altered Metabolism and Bio-markers.....	15
3.2	Structural and Functional Changes	15
3.3	Site of Presentation	16
3.4	Factors related to DFU development	16
3.5	Stages of the Disease.....	23
4	Diabetic Ulcers: Diagnostic and Prognostic Factors.....	27
4.1	Clinical Examination.....	27
4.2	Traditional Tests	29
4.2.1	Diabetic foot and vascular ultrasound.....	29
4.2.2	PHOOTONICS diagnostic imaging protocol	39
4.3	Complementary tests.....	39
5	Photonics Based Diagnostic Tests	42
5.1	Thermal imaging and Long IR spectrum	43
5.1.1	Medical Infra-Red Imaging Fundamentals	43
5.1.2	Medical Infra-Red Images for diabetic foot ulceration.....	43
5.1.3	Comparisons	48
5.2	Hyperspectral and NIR Spectrum Technologies.....	49
5.2.1	Medical Hyperspectral Imaging Fundamentals	49
5.2.1.1	Acquisition Mode	50

5.2.1.2	Spectral Range	50
5.2.1.3	Measurement mode	50
5.2.1.4	Detector	50
5.2.1.5	Dispersive device	51
5.2.2	Medical Hyperspectral Images in Diabetic Foot	51
5.2.3	Comparisons	55
5.3	Mid-IR Spectrum Technologies	56
6	Suggested photonic oriented clinical indexes for diabetic ulcer management	58
	References	61

Figures

Figure 2-1: Forest plot of comparison: Male gender, outcome: DFU development	10
Figure 2-2: Forest plot of comparison: Age, outcome: DFU development	10
Figure 2-3: Forest plot of comparison: Lives alone, outcome: DFU development.....	11
Figure 3-1: Forest plot of comparison: History of DFU, outcome: DFU development.....	18
Figure 3-2: Forest plot of comparison: Duration of diabetes, outcome: DFU development.....	19
Figure 3-3: Forest plot of comparison: History of Cerebrovascular Accident (CVA), outcome: DFU development.....	19
Figure 3-4: Forest plot of comparison: Visual impairment, outcome: DFU development	19
Figure 3-5: Forest plot of comparison: Peripheral Artery Disease (PAD), outcome: DFU development ...	20
Figure 3-6: Forest plot of comparison: Insulin use, outcome: DFU development.....	20
Figure 3-7: Forest plot of comparison: Level of HbA1C, outcome: DFU development	20
Figure 3-8: Forest plot of comparison: Foot deformity / Charcot osteoarthropathy, outcome: DFU development.....	21
Figure 3-9: Forest plot of comparison: Onychomycosis, outcome: DFU development	21
Figure 3-10: Forest plot of comparison: altered Semmes-Weinstein monofilament (SWM) test results, outcome: DFU development	21
Figure 3-11: Forest plot of comparison: History of lower extremity amputation, outcome: DFU development.....	22
Figure 3-12: Forest plot of comparison: Foot oedema, outcome: DFU development	22
Figure 3-13: Forest plot of comparison: Claudication, outcome: DFU development.....	22
Figure 4-1 Lesions such as fungal infection, cracks and skin fissures, deformed nails, macerated web spaces, calluses,	27
Figure 4-2 The suggested frequency for follow-up based on expert consensus	29
Figure 4-3 Vascular laboratory criteria of peripheral artery stenosis [40].....	31
Figure 4-4 MRA compared to contrast angiography is a less invasive imaging technique.	32
Figure 4-5 MRA and CTA roadmap for the same patient	35
Figure 4-6 DSA and QUISS MRA for tibial and pedal arteries of the same patient	36
Figure 4-7 CTA road map, 3-D technique	37
Figure 5-1 Example of thermal imaging [18]	42
Figure 5-2 Classification of hyperspectral HSI systems based on acquisition mode [68].....	49
Figure 5-3 Detector examples in HSI	51

Tables

Table 3-1: The WIFI classification system of foot ulceration	26
Table 4-1 Clinical examination parameters taken into consideration for diabetic foot	28
Table 4-2 Availability, cost, operator expertise, diagnostic accuracy for DSA, CTA, MRA in LEAD diagnosis	33
Table 4-3 Comparison of different imaging tests for patients with LEAD.....	38
Table 5-1 Summary of Literature: Review Table of the Published Works Related to DF Diagnosis with Infrared Thermography.....	43
Table 5-2. Spectral Range Examples in HSI Systems	50
Table 5-3 Summary of Literature: Review Table of the Published Works Related to DF Diagnosis with Hyperspectral Images.....	51
Table 5-4. HSI Systems Characteristics in Diabetic Foot Ulceration.....	56
Table 5-5. Summary of Literature: Review Table of the Published Works Related to DF Diagnosis with RGB Or Mid-IR Images.....	56
Table 6-1. Outcomes for Photonics Based Diagnostic Tests	59

1 Introduction

Diabetic foot disease results in a heavy burden on the patient and the healthcare system. According statistical predictions, nearly 600 million people worldwide will be diabetic in 2035. From these, about 50% are expected to develop peripheral neuropathy and 15–25% are estimated to present one or more foot ulcers (1).

Diabetic foot disease is related to a high morbidity and mortality being a common cause of hospitalization in diabetic patients. Patients with diabetes have a lifelong risk of developing a foot ulcer between 15% and 25%, with an annual incidence of around 2%. The risk for a lower extremity amputation is 23 times higher than in a non-diabetic person. In 2010–2011 in England and Wales there were 72 459 hospital admissions for diabetes-related foot complications, at an estimated cost of between £639 million and £662 million to the National Health Service (2).

In 2007, the United States spent 174 billion dollars for diabetes and its complications. The estimated cost of treating a foot ulcer was approximately €10K in one large European study (3).

It is worthwhile to mention that for each euro spent on ulcer prevention, ten more euros are spent on ulcer healing, and that for each randomized controlled trial focused on prevention, ten trials are conducted on healing.

Foot ulcers are a major risk factor for foot infection and amputation. Furthermore, foot ulcers reduce patient mobility and quality of life. Therefore, by far the most effective way to avoid the enormous cost and the devastating complications of DFU is by preventing the foot ulcer.

In prospective studies a very high risk for recurrent ulcerations has been observed. Reported ulcer recurrence rates are 30–40% in the first year after an ulcer episode, compared with 7.5% annual incidence for patients with peripheral neuropathy but no ulcer history.

However, foot ulcer prevention receives little attention, both in clinical practice and in scientific research (1).

The etiology of DFU is multifactorial. Distal polyneuropathy (motor, sensory and autonomic), foot deformity, functional changes in the microcirculation and PAD contribute to DFU development. The process to ulceration starts by an abnormal pressure exposure or trauma to the often painless diabetic foot. Neuropathy and peripheral arterial disease (PAD) impair healing, while the demand for oxygen is increased by ulceration and infection. The wound healing process may be further delayed by various biological factors inherent to diabetes, such as impaired humoral immunity and abnormal inflammatory response.

PAD is an independent risk factor for foot ulcer and amputation in diabetes. It is present in about 50% of patients with diabetic foot ulcer. In the presence of PAD, ulcer healing is less likely to occur and the risk of amputation increases compared to patients without PAD. Therefore, it is important that all patients with diabetes are tested for PAD.

The diagnosis of PAD in diabetic patients may be overlooked because symptoms and signs are often masked by diabetic distal symmetrical polyneuropathy. Another reason for this may be that many patients with DFU are treated by primary care physicians, podologists or specialists in internal medicine who are not as familiar with the diagnosis of PAD as angiologists or vascular surgeons. According to the International Working Group for Diabetic Foot (IWGDF) guidelines, in addition to a thorough history for symptoms of PAD, all patients with a diabetic foot ulcers should be evaluated by hand-held Doppler for both pedal pulses and measurement of ABI. In cases of diagnostic uncertainty, measurement of toe-brachial index (TBI) or transcutaneous pressure of oxygen (TcPO₂) is suggested. Those patients with signs and symptoms of PAD,

including claudication, rest pain, absent foot pulses, monophasic Doppler signals, ABI <0.9 or TBI <0.7 should be referred to a vascular department for imaging of the vascular tree and for planning potential revascularization procedures in an interdisciplinary approach. With respect to ankle pressure measurements, an ABI of <0.6 is suggestive of severe obstructive arterial disease and a significant impairment in wound healing (2).

Duplex sonography (practically the combination of pulsed Doppler sonography with real time B mode ultrasound imaging and color Doppler scanning) is a non-invasive, reliable, user friendly imaging modality of peripheral vessels. The method detects the Doppler flow patterns in a defined area within the vessel lumen, and within arterial stenoses. Stenosis is scaled by the ratio between the peak systolic velocity of the target/stenosed vessel and the adjacent or the contralateral non-stenosed vessels. This ratio is called peak systolic velocity ratio (PSVR).

In cases of severe arterial stenosis, the traditional contrast angiography, the computed and the magnetic resonance angiography remain the most widely performed imaging techniques. All of these tests aim to determine regional foot perfusion and, if necessary, guide vascular interventions in patients with significant limb ischemia and foot ulceration.

Diabetic peripheral neuropathy eventually develops in nearly 50% of diabetic patients. It is associated with increased morbidity including pain, foot ulcers, and lower limb amputation. The prevalence of peripheral neuropathy is estimated to be between 6% and 51% among adults with diabetes and increases with age, duration of diabetes, poor glycemic control, and type 1 versus type 2 diabetes. Diabetic peripheral neuropathy (DPN) is defined as, “the presence of symptoms and/or signs of peripheral nerve dysfunction in people with diabetes after the exclusion of other causes”. The diagnosis of DPN is based on both clinical signs and on quantitative testing. There are two types of diabetic peripheral neuropathy. Diabetics are commonly affected by distal symmetric polyneuropathy. Mononeuropathies are atypical forms of DPN. Apart from age, duration of diabetes and poor glycemic control, DPN is also associated with atherosclerotic cardiovascular disease and cardiovascular risk factors such as hyperlipidemia, obesity, smoking, and hypertension.

Elevated levels of dynamic plantar pressure while walking have been identified as a significant risk factor for incident and recurrent diabetic plantar foot ulcers. Unfortunately, a plantar pressure threshold below which foot ulceration occurs with certainty has not been identified to date. On the other hand, plantar pressure measurements are useful for preventive recommendations and for the design of off-loading footwear for high-risk diabetic patients.

Elevated plantar pressure results in increased plantar skin temperature. This rise of temperature is due to inflammation and to enzymatic autolysis of plantar tissue that is mildly or moderately stressed during walking. The value of infrared thermometry in foot ulcer prevention has been assessed in several randomized controlled trials. The aim of these studies was to investigate possible associations between the increased local temperature and foot ulceration. Absolute temperature values or comparisons of temperature between regions of the same foot may not be reliable indicators. A 2.2 °C difference between corresponding regions of both feet may be used as a threshold for the patient to reduce ambulatory activity and pressure exposure. With advanced infrared imaging using high-resolution infrared cameras, temperature profiles of the foot can be studied in more detail than with handheld thermography (4).

A history of foot ulcer, DPN, structural foot deformities, elevated local plantar pressure, rise of local foot temperature, PAD, visual impairment, diabetic nephropathy, poor glycemic control, and smoking are the most powerful risk factors for the development of diabetic foot ulcer.

2 Diabetic Ulcers: Epidemiology

2.1 Distribution over European Populations

Over 55 million Europeans suffer from diabetes, or about 10.3% of men and 9.6% of women aged 25 years or over. Prevalence of diabetes is increasing among all ages in the European region, mostly due to increases in overweight and obesity, unhealthy diet and physical inactivity. Diabetes is the most common underlying cause of foot ulcers, infections, ischemia, and amputations in the United States and Europe. The incidence of diabetic foot has increased in parallel with the worldwide prevalence of DM and the prolonged life expectancy of diabetic patients. A large population-based study from three district hospitals in the UK confirmed that 1.4% of type 2 diabetic patients had active DFU and 5% had ever had ulcers (5). Other studies demonstrated that 2-4% of the patients with diabetes present a DFU, while the risk of developing DFU during their lifetime could be as high as 25% (6, 7). The annual incidence of DFU is reported around 2% (8, 9). Today, approximately 8 million of diabetic patients in Europe are at risk of developing a diabetic foot ulcer (DFU).

DFU can lead to severe damage on the foot resulting in extremity amputation. DFU is important because 80-85% of all diabetic lower extremity amputations, both major and minor, are preceded by an ulcer (10). A previous study has shown that every 30 seconds a lower limb is amputated due to diabetes (11). The incidence of ulceration and amputation has declined in Sweden and the Netherlands and appears to be leveling off in Germany and Great Britain (12, 13). Patients with diabetes that suffer a DFU will face severe morbidity with a 20-fold higher risk of amputation compared to non-diabetic patients (14, 15). The survival rates at 3 years following an amputation are worse than the survival rates of cancer patients: for foot amputation survival rate at 3 years is 54%, for leg amputation 44% and for thigh amputation 30%. In dialysis amputees even 1-year survival rate is only 50.8% (16, 17).

In a systematic review (18) that included a large sample of patients involving more than 800,000 global participants from 67 studies of the past three decades, the prevalence of DFU in Europe was 5.1%. The overall prevalence in Europe is lower than in North America (13%), Africa (7.2%) and Asia (5.5%) but higher than in Oceania (3%). Data from various European countries demonstrated the following prevalence rates of DFU: Belgium 16.6%, Norway 10.4%, Italy 9.7%, Denmark 7.8%, UK 6.3%, France 5.6%, Greece 4.8%, Ireland 3.9%, Spain 3%, Germany 2.8%, Netherlands 1.8%, and Poland 1.7%.

In conclusion, DFU represents a significant cause of morbidity worldwide and also in European countries. The prevention and early detection of DFU is important to decrease the numbers of affected patients and to diminish the detrimental consequences associated with the disease.

2.2 Demographics

Although DFU are preventable by multiple measures, they represent more than 50% of the causes of hospital admissions in patients with DM (7). Diabetic foot problems are recognized as a serious public health problem.

The risk of foot lesions increases with both age and duration of DM. Male patients have a 1,6-fold increased risk to develop ulcers compared with female patients (7, 19). Ethnicity also seems to influence the prevalence of DFU since Europeans show a higher risk than patients from India, Asia or Africa (20).

Trying to identify the risk factors that are related to the development of DFU we performed a systematic review of the literature (21-29) (see section 3.4). Demographic data including gender, age, and lifestyle were examined in diabetic patients who developed or who did not develop DFU. The results were the following:

Male gender: Male patients presented a trend towards higher incidence of DFU but the difference was not statistically significant as compared to female patients (OR 1.33, 95% CI: 0.89 – 1.98).

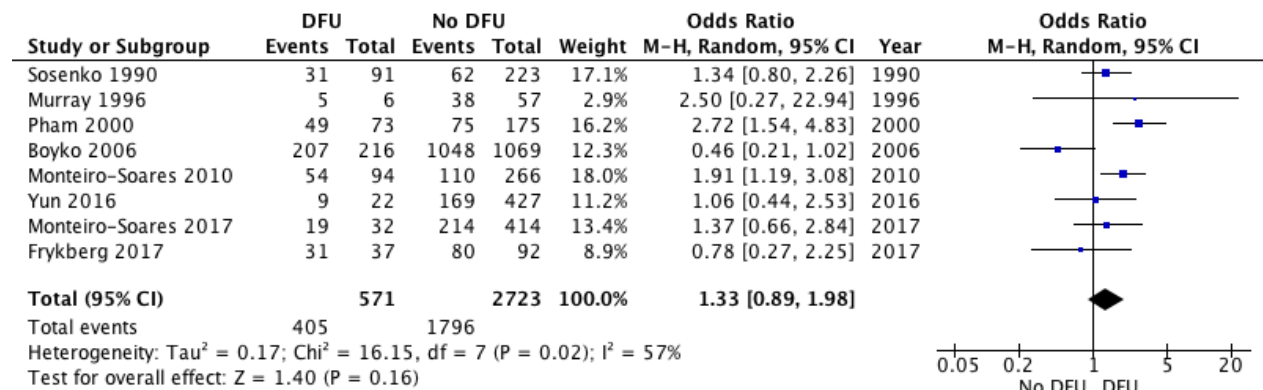


Figure 2-1: Forest plot of comparison: Male gender, outcome: DFU development

Age: No statistically significant difference was found between those diabetic patients who developed and those who did not develop a DFU (mean difference 0.31 years older those who developed a DFU, 95% CI: -0.77 – 1.39).

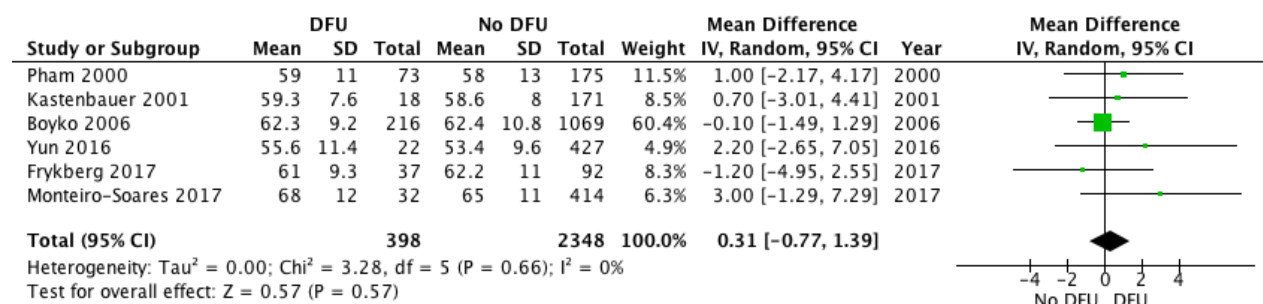


Figure 2-2: Forest plot of comparison: Age, outcome: DFU development

Living alone: Finally, living alone was not related to the development of DFU (OR 0.79, 95% CI: 0.40-1.57).

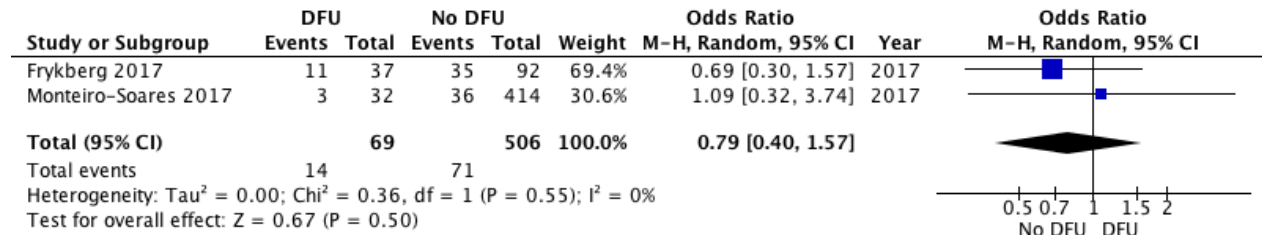


Figure 2-3: Forest plot of comparison: Lives alone, outcome: DFU development

2.3 Associated Risks Factors

The etiology of DFU is complex, and an ulcer is rarely the result of a single factor. DFUs are caused by a combination of (1) autonomic, motor, and sensory neuropathy; (2) abnormal foot mechanics, leading to increased pressure and shear; (3) structural foot deformities coupled with limited joint mobility, which amplify the effects of neuropathy; (4) PAD; (5) trauma; and (6) poorly fitting shoes (30, 31). Heel ulcers, for example, commonly have two essential components: gravitational (decubitus) pressure transmitted to the heel, and ischemia (32). In general, foot ulcers are the cumulative result of too high pressure exposure and repetitive trauma.

The major underlying conditions that are mostly associated with diabetic foot problems are neuropathy and lower limb ischemia (peripheral artery disease, PAD). Neuropathy is found in 90% of DFU, especially in patients in late stages of the disease, because they lack the „gift of pain”, being not capable to protect themselves from repetitive minor trauma(33). Patients with diabetes have a 2 to 4 fold risk of developing PAD and the majority of patients have no vascular symptoms until they develop tissue loss(34-36). In high and middle income countries 50% of patients with DFU have PAD, whereas in low income countries neuropathic ulcers seem predominant (19, 20, 37, 38).

DPN affects up to 50% of patients with DM and is defined as symptoms and signs of peripheral nerve dysfunction in people with diabetes, after exclusion of other causes (39, 40). Patients with DPN experience a wide spectrum of symptoms ranging from a painful form (electrical sensations, stabbing, stinging pain, burning/freezing sensation) exacerbated during the night to numb sensations that begin in the toes and allodynia (pain exacerbated by a neutral stimulus on hyperaesthetic skin in the feet).

Semmes Weinstein 10 g monofilament test (SWM) is the gold standard for identifying loss of protective sensation in the feet of patients with DPN. Inability to feel 10 g monofilaments predicts a 15 fold risk of developing a DFU (41).

DPN is associated with small muscle atrophy in the feet and below the knee. This explains reduced or absent reflexes and imbalance of flexor/extensor motor function responsible for deformities like clawing of the toes. Sensory dysfunction due to DPN is translated into altered proprioception and reduced joint position sensation with subsequent adaptation in motor response. All these alterations are causing unsteadiness while standing associated with increased risk of falls and depression.36

Sympathetic autonomic neuropathy leads to variable degrees of microvascular dysfunction. Loss of

sympathetic tone results in increased arteriolar flow to the foot, with concomitant capillary (skin) ischemia due to pre-capillary vasoconstriction and increased venous flow with distended veins on skin surface. The lower limb is warm and insensate due to DPN. Besides loss of hair follicles, the reduction of sweating activity causes dry skin and promotes callus formation(42).

PAD has a characteristic pattern in patients with DM, when compared to patients that do not have DM. PAD in diabetic patients occurs at a younger age and the location of the disease is more distal, multi-segmental and bilateral. Further attributes include medial calcification, impaired collateral formation and faster progression with higher risk of amputation (43).

A valuable measurement to define PAD (95% sensitivity and 100% specificity) is an ankle-brachial index (ABI) or ankle-arm index (AAI) below 0.9. However, due to calcified arteries below the knee, which is a common feature in patients with DM and/or end-stage renal disease – ABI may be falsely elevated, above 1.4 (sensitivity and specificity decreases below 50-70% and 30-96.8%, respectively) (44). In order to prevent misclassification it is sometimes useful to measure the toe-brachial pressure index, with abnormal values below 0.7. According to the current evidence a patient with a DFU and PAD has poor chances of healing and increased risk of amputation if the toe pressure is below 30 mmHg and/or TcPO₂ is lower than 25mmHg(45, 46).

Intermittent claudication is the cardinal symptom of PAD. It is defined as pain from muscle ischemia when walking and it is experienced at buttocks, thighs or calves, according to the level of arterial obstruction. It is estimated that almost between 50% and 65% of the patients with decreased ABI are asymptomatic. However, one third of them may develop symptoms during 6 min walking test(47, 48). In contrast, the majority of patients with DM lack intermittent claudication as the first symptom of PAD (49, 50).

Neuropathy (inability to feel a 10 g monofilament), PAD (at least one absent pedal pulse) and history of foot ulceration were used to generate a reliable model for the predicting the risk of diabetic foot ulceration with data obtained from a meta-analysis of over 16 000 patients (51).

Other frequently occurring risk factors of foot ulcers are:

Renal failure: patients with DM that receive dialysis have a higher risk of developing a FU. There has been found a direct temporal association between the initiation of dialysis and the risk of foot ulceration (52-54).

Callus formation is the consequence of combined raised pressure on the foot and of the sympathetic autonomic neuropathy and it is associated with 11 fold-increased risk of DFU (52-54). Patients with callus have 2.4 more frequent higher foot pressures, mostly in the plantar forefoot area. The estimated threshold of plantar pressure with clinical significance seems to be 87.5N/cm² (sensitivity 63.5%; specificity 46.3%). Patients with plantar pressures higher than 87.5N/cm² were twice as likely to develop an ulcer during next 2 years (31). Plantar pressure increases with numbers of deformities as hallux valgus (bunion), hallux limitus, clawing of the toes(55). In short, foot pressures are higher in the presence of neuropathy, deformity, callus, previous DFU, or amputation.

Peripheral oedema is another frequent factor that adversely affects local blood flow and associates with increased risk of foot complications (56).

There is an overwhelming evidence that a previous ulcer or amputation confers a 3-78 fold higher risk of future foot problems and that between 30 and 40% of patients with a DFU will experience another ulcer in the year after healing (57).

Probably a combination of integral time of pressure (time spent at the point of high pressure), activity level

(no of repetitions at the point of high pressure/unit of time) and shear forces that set up an unperceived tissue trauma in the presence of neuropathy and PAD are the major pathophysiologic risk factors for foot ulceration.

2.4 Current diagnostic/treatment cost and management

The annual cost of DFU is on average 8659 \$ per patient globally (58). Different other studies report significant costs related to foot problems: 580 million £ in UK, during 2010 and 2011, representing 0.6% of the NHS expenses during that period of time and over 17 billion \$ annually in the US for the care of about 1.7 million DFU patients (59-61).

Not surprisingly, the cost of diagnosis and treatment of patients with DFU is increased as compared to patients without DFU. In a retrospective study among diabetic patients in a tertiary hospital in Turkey (62), 203 patients with type 2 DM (91 with DFU, 122 without) the average hospital cost of patients with DFU was calculated as 976.1 ± 253.6 USD per person as compared to 430.3 ± 144.2 USD per person of patients without. Similarly, there were significant differences between the groups on costs of drugs, equipment and services.

In 2007, the treatment of diabetes and its complications in the United States generated at least 116 billion USD in direct costs, with at least 33% of these costs attributable to DFU (3). A retrospective nested case-control study demonstrated that the relative cost of care for diabetic patients with lower extremity ulcers ranges from 1.5 to 2.4 times higher than that of diabetic patients without an ulcer in the year before diagnosis to 5.4 times higher in the year after the ulcer episode (61). Even after healing, treatment cost of diabetic patients with a former ulcer was 2.8 times higher than treatment cost of diabetic patients without ever having had an ulcer (63).

In a large inpatient sample in US hospitals between 2005-2010, the outcome and per-admission cost among patients with DFU versus patients with non-DM ulcers was investigated (64). In about 1 million patients with foot ulcers admitted over the study period, the overall rate of admissions was relatively stable over time, nevertheless the ratio of DM versus non-DM admissions increased significantly (from 10.2 in year 2005 to 12.7 in 2010, $p < 0.001$). Similarly, the admissions related to infection rose significantly among DM patients, but remained stable among non-DM patients.

It is clear that the cost of care for diabetic patients with a lower extremity ulcer causes additional major economic burden compared with the management of a patient with diabetes but no ulceration. Extensive patient education, early detection and assessment and aggressive treatment by a multidisciplinary team represent the best approach to manage these patients. Early assessment of the risk for DFU and preventive measures to reduce the incidence of DFU are essential. Education initiatives and early prevention strategies through outpatient care targeted at high-risk populations are instrumental to prevent further increases in cost of care.

2.5 The Impact of early diagnosis and follow up in efficient diabetic ulcer management

The International Diabetes Federation (IDF) report that every 20 seconds somebody with diabetes suffers limb amputation. It is estimated that 85 % of all amputations caused by diabetes are preventable if early detected and treated.

Serious diabetic foot complications can be delayed and even prevented with appropriate, careful, and reliable screening and management standards. Several countries and organizations such as WHO and IDF have made suggestions with the aim of reducing the rate of amputations by up to 50%. It is speculated that implementing a foot screening and protection program for patients at risk of ulceration may reduce both morbidity and cost (65). However, a diabetic foot-screening tool needs to be evidence-based (66). Since there are advances in technology, biomechanical modelling, and treatment innovations, it is relevant to also improve current foot screening guidelines to prevent amputations and to preserve limb function in high-risk patients.

Early detection of a DFU is crucial to provide prompt care and reduce the risk of amputation. In clinical routine, regular foot checks are often neglected. It is estimated that only 30 to 60% of the patients with diabetes get a frequent foot screen. Multiple factors may account for this low rate with patients not liking showing their feet, time constraints by physicians etc. Guidelines for diabetic patients recommend that on in addition to the annual diabetes foot screen, all people with high risk for DFU, particularly with neuropathy, should have their feet checked every time they see a health professional. Additional risk factors include obesity, age, and vision impairment.

Treatment of patients with diabetes should include screening for peripheral neuropathy, peripheral vascular disease (PAD), and foot deformation, evaluation of joint mobility, and inspection of footwear.

In addition to foot screening and control as suggested by several diabetes guidelines (67), standardized protocols for simple self-assessment of the feet may be very helpful in the prevention of DFU.

3 Diabetic Ulcer pathophysiology

3.1 Altered Metabolism and Bio-markers

More than 60% of diabetic foot ulcers are caused by neuropathy (68, 69). Neuropathy has been shown to result from hyperglycemia-induced metabolic abnormalities in animal and in vitro models (70-72). Postulated pathophysiologic mechanisms for the development of neuropathy include the polyol pathway (70). In the development of neuropathy, the hyperglycemic state leads to an increase in action of the enzymes aldose reductase and sorbitol dehydrogenase. This results in the conversion of intracellular glucose to sorbitol and fructose. The accumulation of these sugar products results in a decrease in the synthesis of nerve cell myoinositol, which is required for normal neuron function. Additionally, the chemical conversion of glucose results in a depletion of nicotinamide adenine dinucleotide phosphate stores, which are necessary for the detoxification of reactive oxygen species and for the synthesis of the vasodilator nitric oxide. There is a resultant increase in oxidative stress on the nerve cell and an increase in vasoconstriction leading to ischemia, which will promote nerve cell injury and death. Hyperglycemia and oxidative stress also contribute to the abnormal glycosylation of nerve cell proteins and inappropriate activation of protein kinase C, resulting in further nerve dysfunction and ischemia (68).

Diabetic neuropathy affects the motor, autonomic, and sensory components of the nervous system(68). Impaired innervation of the intrinsic foot muscles leads to an imbalance between flexion and extension of the affected foot. This produces anatomic foot deformities causing pressure points, which increase the risk of ulceration.

Autonomic neuropathy leads to reduced perspiratory gland function. As a result, the foot becomes increasingly dry and therefore more susceptible to tears with subsequent infection.

The loss of sensation as part of DPN aggravates the development of ulcerations. Many wounds also remain undetected and progressively increase in size because they are continuously exposed to pressure and shear forces (73).

Peripheral arterial disease (PAD) is^[1] a contributing factor to the development of foot ulcers, present in up to 50% of cases (32, 74). It commonly affects the tibial and peroneal arteries of the^[1] calf. Endothelial cell dysfunction and smooth cell abnormalities develop in peripheral arteries as a consequence of the persistent hyperglycemic^[1] state (72). There is a resultant decrease^[1] in endothelium-derived vasodilators leading to constriction. Moreover, the hyperglycemia in diabetes is associated with an increase in thromboxane A₂, a vasoconstrictor and platelet aggregation agonist, which leads to plasma hypercoagulability (75). There is also the potential for alterations in the vascular extracellular matrix leading to stenosis of the arterial lumen (75). Moreover, smoking, hypertension, and hyperlipidemia are other factors that are common in diabetic patients and contribute to the development of PAD (76). Cumulatively, this leads to occlusive arterial disease causing ischemia of the lower extremities and an increased risk of ulcerations in diabetic patients.

3.2 Structural and Functional Changes

The development of foot ulcers is often a result from poor biomechanics (30, 31, 77). Ulcer prevention requires attention to this pivotal and often misunderstood component of pedal energy transfer. Shear and stress develop on the sole of the foot at the site of high pressures resulting from structural foot deformity and limited joint mobility. Structural deformities such as claw toes, hallux valgus, dislocated metatarsophalangeal joints, and limited motion of the ankle and first metatarsophalangeal joint are

regularly associated with foot ulcers. Dorsiflexion of the ankle joint should be 10 degrees from neutral, and dorsiflexion of the first metatarsophalangeal joint should be about 50 degrees from neutral. A combination of clawing of the toes and dislocation of the metatarsophalangeal joints causes retrograde buckling and dislocation. These forces cause the toes to be dislocated dorsally and the metatarsal head to be pushed in a plantar direction which leads to severe pressure exposure of the skin in this areas.

The importance of bone deformities that expose the overlying skin to trauma cannot be overemphasized. Because diabetics with neuropathy lack normal sensation, they may also select shoes that are too small. In addition, progressive deformities (e.g. hammertoe) may require patients to purchase ill-fitting shoes that are wider and deeper than needed in the past. Because of DPN, patients may sustain penetrating injuries such as lacerations and puncture wounds that are not recognized owing to the loss of protective sensation.

3.3 Site of Presentation

DFUs can develop at any part of the feet, ankles, or toes. Claudication and rest pain occur less often in diabetics with neuroischemic ulceration than in non-diabetics with purely ischemic lesions; ulcers overlying the medial and lateral malleoli and metatarsophalangeal joints may cause pain despite neuropathy and the absence of infection because of penetration to the bone.

Ulcers on the great toe often develop because of arthritis or limited motion of the first metatarsophalangeal joint. At toe-off in gait, the reduced motion causes more pressure and shear forces under the first metatarsal head or at the interphalangeal joint of the great toe. Ulcers on the tips of claw toes usually arise because of constant pressure and weight bearing. Bony prominences in the midfoot and unilateral flatfoot often result from Charcot's neuro-osteoarthropathy, neuropathic fracture, or a tear of the posterior tibialis tendon; these areas may ultimately become sites of ulceration. Classically, ulcers on the metatarsal heads (the "ball" of the foot) occur at sites of high pressure and shear forces that are exposed to repetitive injury (normal walking). In the presence of sensory neuropathy, a normally painful damage to soft tissues is not recognized until an ulcer develops and is detected by inspection or malodor rather than by pain. Ulcers on the dorsum or sides of the foot are usually due to ill-fitting shoes.

3.4 Factors related to DFU development

Various clinical indices have been related to the development of DFU. However, the quality of studies and corresponding data varies. We made a systematic review of the literature trying to identify the clinical factors that have been related to DFU development.

The Medline database was searched using the PubMed software. The search terms used were the following: diabetic AND (ulcer OR ulceration) AND prediction AND (lower limb OR foot OR lower extremity) and included the period from 1976 to 2020.

All data sets were prepared for meta-analysis in the same way, following a list of rules and exclusion criteria. The review included studies that contained data from individuals who were free of foot ulcers at the time of study entry and who had the diagnosis of diabetes mellitus. Patients had to be followed for various time periods until some of them developed foot ulceration. Studies had to include information regarding various potential predisposing factors (variables) for the development of foot ulceration. Variables for meta-analysis were selected if they were included in at least three studies. Studies that included patients with foot ulcer at the time of study entry were excluded.

We chose the random-effects meta-analysis, which does not assume that all the estimates from each study are estimates of the same underlying true value, but rather that the estimates belong to the same distribution. The data sets covered a range of temporal, geographical and clinical settings. Therefore, some degree of heterogeneity among studies was expected. Before undertaking any meta-analysis, we assessed the extent of heterogeneity. We employed standard methods of assessing heterogeneity, by examining forest plots of estimates and calculating I^2 and τ -statistics. For the analysis the Review Manager 5 software (v. 5.2.5) was used.

The initial search revealed 176 papers. Among them, 149 were excluded after the abstract and/or full-text reading as irrelevant to the review. Thus, 27 papers remained for data extraction. Among them, 10 papers contained data that satisfied the inclusion and exclusion criteria of our study and were used for the analysis (21-29, 78).

The search revealed the following parameters as possible clinical factors that might predict the development of DFU: age (years), male gender, history of DFU, duration of DM (years), history of cerebrovascular accident, visual impairment, history of lower limb arterial disease, body mass index, insulin use, history of smoking, HbA1C (%), nephropathy, foot deformity / Charcot osteoarthropathy, tinea pedis (athlete's foot), history of lower limb amputation, foot oedema, hyperkeratosis, claudication. Additionally, the following parameters were described but were not analyzed as the number of the referring studies were less than three: living alone habit, arterial hypertension, alcohol consumption, myocardial infarction, retinopathy, physical impairment, adequate skin moisturizing, adequate nail care, rest pain.

The parameters that were referred in more than two studies and analyzed were the following:

- Age: patients with DFU were 0.3 years older than those without but this difference was not statistically significant (95% CI: -0.77-1.39)
- Male gender: more patients with DFU were of male gender, however the difference was not significant (OR 1.33, 95% CI: 0.89-1.98)
- History of DFU: patients who developed a DFU were 3.78 times more likely to have a previous history of DFU and this was statistically significant (95% CI: 1.66 - 8.62)
- Duration of Diabetes Mellitus (DM): the duration of DM was found to be significantly longer in patients who developed a DFU (mean difference 0.30 years, 96% CI: 0.19-0.41)
- History of a cerebrovascular accident (CVA): a history of CVA was more likely in patients who developed a DFU (OR 1.82, 95% CI: 1.03-3.24)
- Visual impairment: patients who developed DFU were more likely to have an impaired vision (OR 3.02, 95% CI: 1.31-6.96)
- History of lower limb arterial disease: a history of peripheral artery disease was more likely in patients who developed a DFU (OR 2.61, 95% CI: 1.40-4.88)
- Body mass index: the body mass index was found to be similar in both groups (mean difference - 0.07, 95% CI: -2.09-1.95)
- Insulin use: patients with insulin were more likely to develop a DFU (OR 2.11, 95% CI: 1.17-3.80).
- History of smoking: smoking was not related to the development of DFU (OR 0.83, 95% CI: 0.62-1.13)
- HbA1C (%): the level of HbA1C was related to the development of DFU. Patients who developed a DFU had a 1.13% (95% CI: 0.21-2.05) higher mean HbA1C level.

- Nephropathy: the presence of neuropathy was not significantly related to the development of DFU (OR 1.81, 95% CI: 0.81-4.00)
- Foot deformity / Charcot osteoarthropathy: the Foot deformity / Charcot osteoarthropathy was related to the development of DFU (OR 2.85, 95% CI: 1.22-6.62)
- Tinea pedis / athlete's foot: tinea pedis was not related to DFU development (OR 0.88, 95% CI: 0.49-1.61)
- History of lower extremity amputation: history of lower extremity amputation was related significantly to the development of the DFU (OR 4.48, 95% CI: 1.70-11.85)
- Oedema: foot oedema was found to be related to the development of DFU (OR 1.47, 95% CI: 1.14-1.88)
- Hyperkeratosis: hyperkeratosis was not related to the development of DFU (OR 1.17, 95% CI: 0.69-1.99)
- Claudication: claudication was related to the development of DFU (OR 1.78, 95% CI: 1.39-2.30).

Overall, the following parameters were related to the development of DFU: history of DFU, duration of DM, history of a cerebrovascular accident, visual impairment, history of lower limbs arterial disease (PAD), insulin use, level of HbA1C, foot deformity (Charcot osteoarthropathy), history of lower extremity amputation, foot oedema, claudication, onychomycosis, altered Semmes-Weinstein monofilament (SWM) test results.

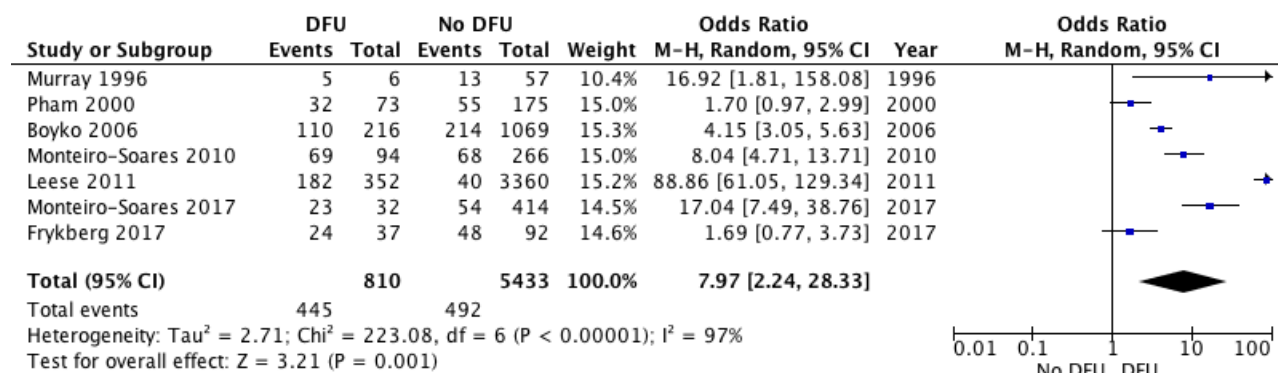


Figure 3-1: Forest plot of comparison: History of DFU, outcome: DFU development

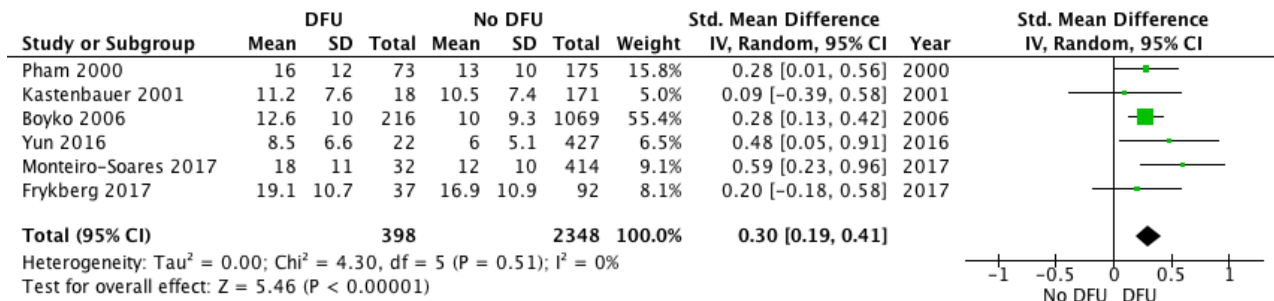


Figure 3-2: Forest plot of comparison: Duration of diabetes, outcome: DFU development

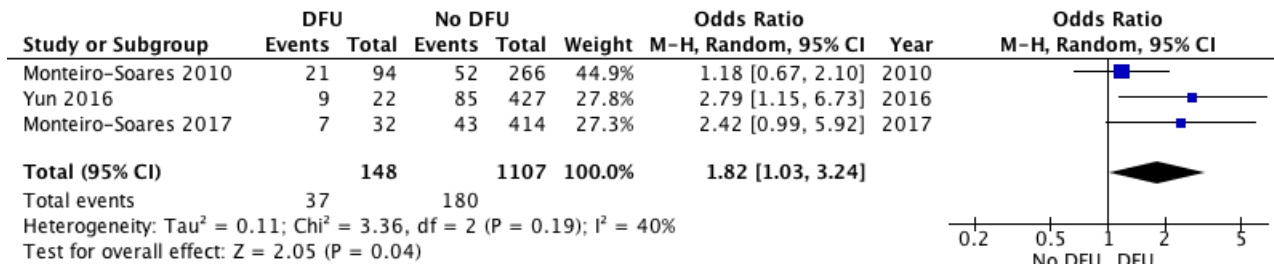


Figure 3-3: Forest plot of comparison: History of Cerebrovascular Accident (CVA), outcome: DFU development

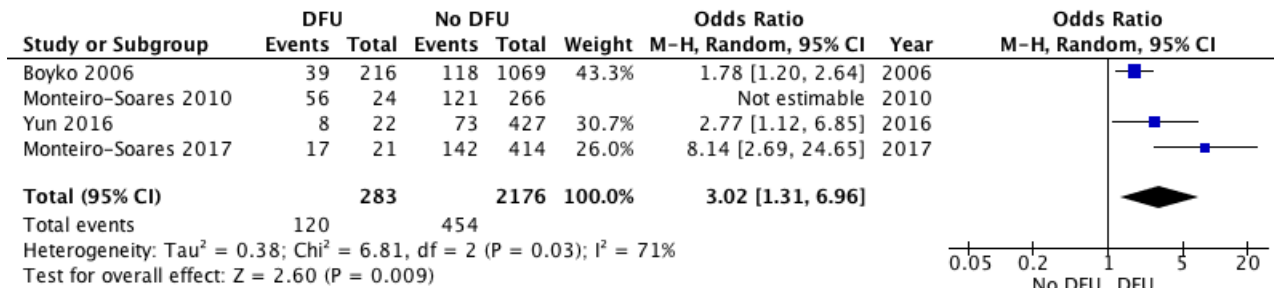


Figure 3-4: Forest plot of comparison: Visual impairment, outcome: DFU development

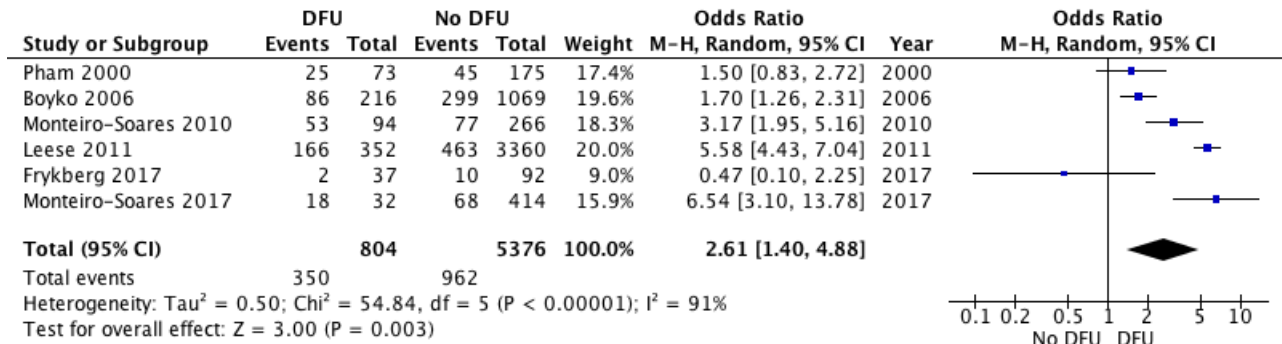


Figure 3-5: Forest plot of comparison: Peripheral Artery Disease (PAD), outcome: DFU development

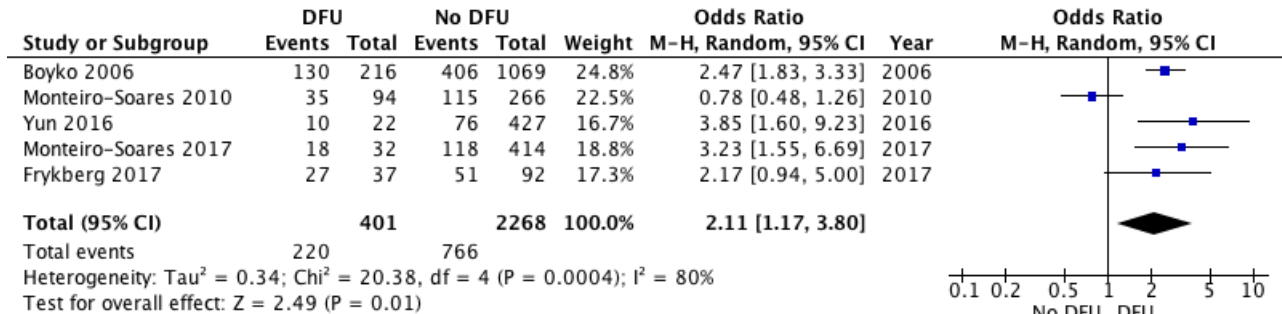


Figure 3-6: Forest plot of comparison: Insulin use, outcome: DFU development

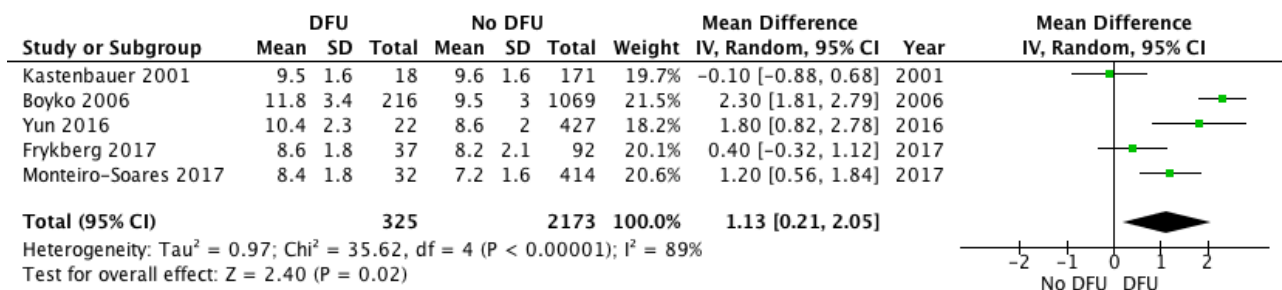


Figure 3-7: Forest plot of comparison: Level of HbA1C, outcome: DFU development

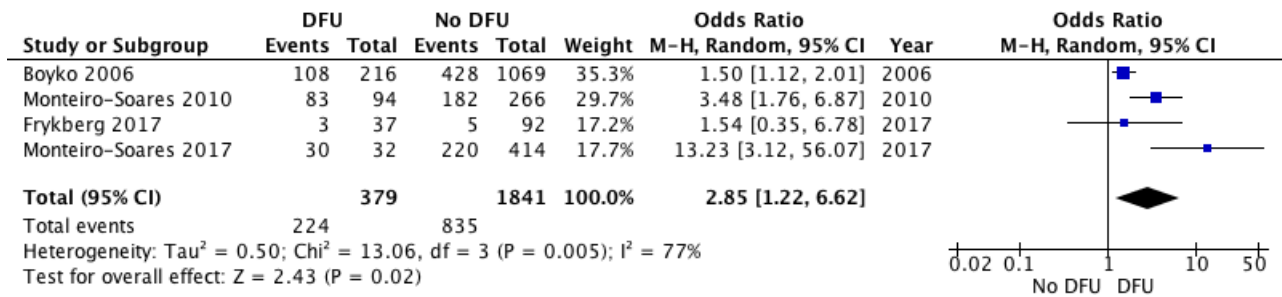


Figure 3-8: Forest plot of comparison: Foot deformity / Charcot osteoarthopathy, outcome: DFU development

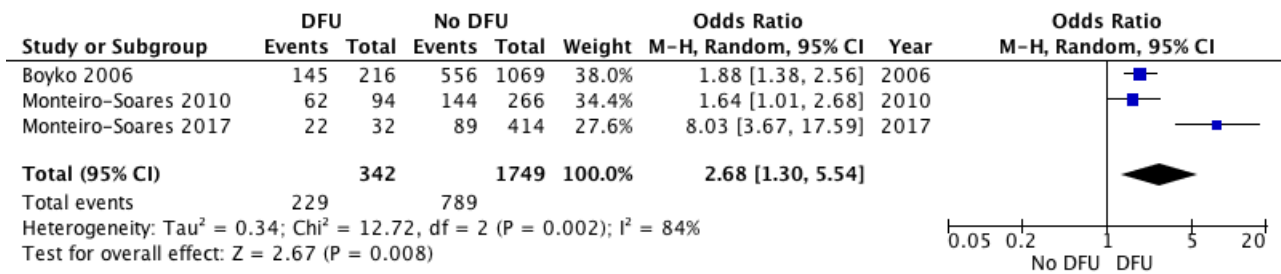


Figure 3-9: Forest plot of comparison: Onychomycosis, outcome: DFU development

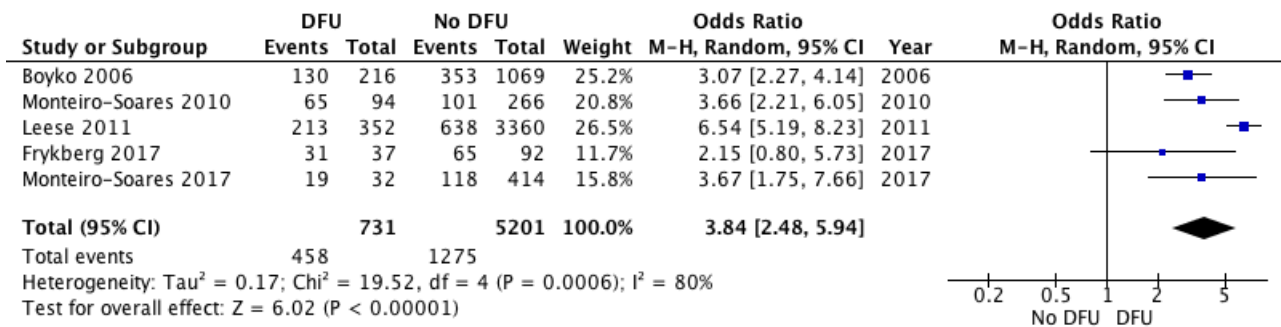


Figure 3-10: Forest plot of comparison: altered Semmes-Weinstein monofilament (SWM) test results, outcome: DFU development

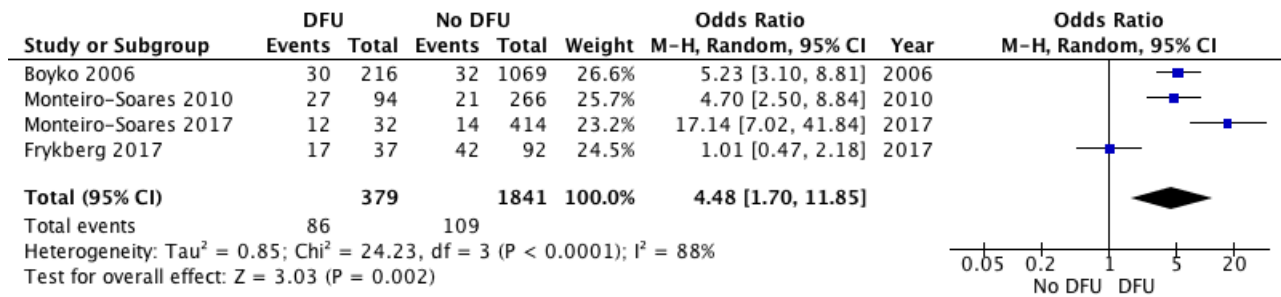


Figure 3-11: Forest plot of comparison: History of lower extremity amputation, outcome: DFU development

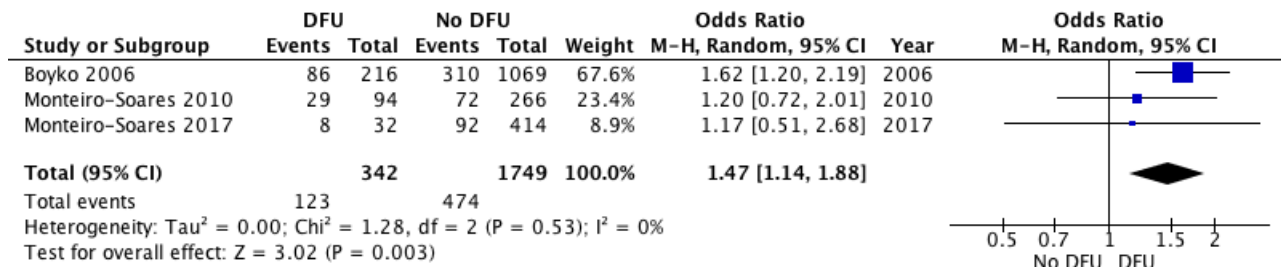


Figure 3-12: Forest plot of comparison: Foot oedema, outcome: DFU development

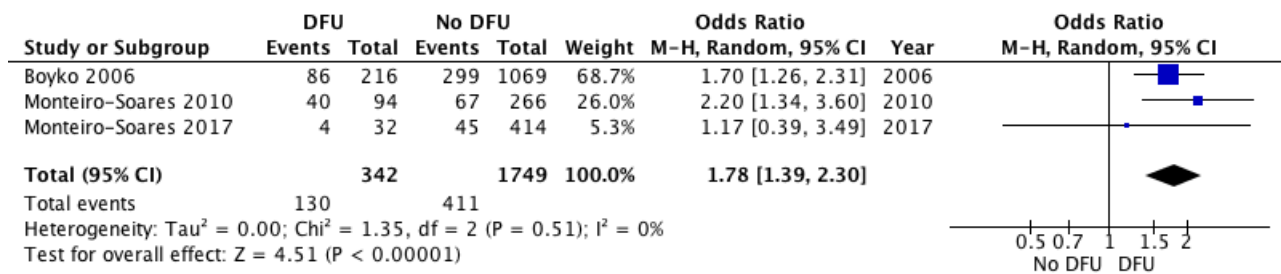


Figure 3-13: Forest plot of comparison: Claudication, outcome: DFU development

3.5 Stages of the Disease

It is crucial to apply a standardized measurement system to evaluate whether a diabetic foot ulcer is responding to care. Therefore, several classification systems have been proposed.

At the present time no specific system has been universally accepted. Even so, most clinicians use one of the available systems when assessing and documenting a diabetic ulcer.

The Wagner Diabetic Foot Ulcer Grade Classification System

The Wagner diabetic foot ulcer classification system assesses ulcer depth and the presence of osteomyelitis or gangrene by using the following grades:

Grade 0 – intact Skin

Grade 1 – superficial ulcer of skin or subcutaneous tissue

Grade 2 – ulcers extend into tendon, bone, or capsule

Grade 3 – deep ulcer with osteomyelitis, or abscess

Grade 4 – partial foot gangrene

Grade 5 – whole foot gangrene

The University of Texas Diabetic Foot Ulcer Classification System

The University of Texas system grades diabetic foot ulcers by depth and then stages them by the presence or absence of infection and ischemia:

Grade 0 – pre-or post-ulcerative site that has healed

Grade 1 – superficial wound not involving tendon, capsule, or bone

Grade 2 – wound penetrating to tendon or capsule

Grade 3 – wound penetrating bone or joint

Within each wound grade there are four stages:

Stage A – clean wounds

Stage B – non-ischemic infected wounds

Stage C – ischemic non-infected wounds

Stage D – ischemic infected wounds

Nevertheless, most DFU classification systems fail to provide sufficient detail with regard to perfusion status and are ulcer systems with no specific mention of gangrene. Gangrene increases the risk of amputation compared with ulceration. Although the Wagner classification includes gangrene, it does not differentiate gangrene because of infection from that resulting from ischemia. It also fails to characterize the degree of infection, ischemia, or wound extent.

As a result, Society of Vascular Surgery has suggested the WIfI classification (Wound, Ischemia, foot

Infection). According to WIfI, wounds are stratified or graded from grade 0 through grade 3 based on size, depth, severity, and anticipated difficulty achieving wound healing.

The WIfI classification consists of classes and grades as seen in Table 3-1.

W: Wound/clinical category

Grade	Ulcer	Gangrene
0	No ulcer	No gangrene
Clinical description: ischemic rest pain (requires typical symptoms + ischemia grade 3); no wound.		
1	Small, shallow ulcer(s) on distal leg or foot; no exposed bone, unless limited to distal phalanx	No gangrene
Clinical description: minor tissue loss. Salvageable with simple digital amputation (1 or 2 digits) or skin coverage.		
2	Deeper ulcer with exposed bone, joint or tendon; generally not involving the heel; shallow heel ulcer, without calcaneal involvement	Gangrenous changes limited to digits
Clinical description: major tissue loss salvageable with multiple (≥ 3) digital amputations or standard TMA \pm skin coverage.		
3	Extensive, deep ulcer involving forefoot and/or midfoot; deep, full thickness heel ulcer \pm calcaneal involvement	Extensive gangrene involving forefoot and /or midfoot; full thickness heel necrosis \pm calcaneal involvement
Clinical description: extensive tissue loss salvageable only with a complex foot reconstruction or nontraditional TMA (Chopart or Lisfranc); flap coverage or complex wound management needed for large soft tissue defect		

I: Ischemia

Grade	ABI	Ankle systolic pressure	TP, TcPO ₂
0	≥0.80	>100 mm Hg	≥60 mm Hg
1	0.6-0.79	70-100 mm Hg	40-59 mm Hg
2	0.4-0.59	50-70 mm Hg	30-39 mm Hg
3	≤0.39	<50 mm Hg	<30 mm Hg

ABI, Ankle-brachial index; PVR, pulse volume recording; SPP, skin perfusion pressure; TP, toe pressure; TcPO₂, transcutaneous oximetry.

FI: Foot Ischemia

Clinical manifestation of infection	SVS	IDSA/PEDIS infection severity
No symptoms or signs of infection	0	Uninfected
Infection present, as defined by the presence of at least 2 of the following items: <ul style="list-style-type: none"> • Local swelling or induration • Erythema >0.5 to ≤2 cm around the ulcer • Local tenderness or pain • Local warmth • Purulent discharge (thick, opaque to white, or sanguineous secretion) 	1	Mild
<hr/> Local infection involving only the skin and the subcutaneous tissue (without involvement of deeper tissues and without systemic signs as described below).		

Exclude other causes of an inflammatory response of the skin (eg, trauma, gout, acute Charcot neuro-osteoarthropathy, fracture, thrombosis, venous stasis)		
Local infection (as described above) with erythema >2 cm, or involving structures deeper than skin and subcutaneous tissues (e.g., abscess, osteomyelitis, septic arthritis, fasciitis), and No systemic inflammatory response signs (as described below)	2	Moderate
Local infection (as described above) with the signs of SIRS, as manifested by two or more of the following: <ul style="list-style-type: none"> • Temperature >38° or <36°C • Heart rate >90 beats/min • Respiratory rate >20 breaths/min or PaCO₂ <32 mm Hg • White blood cell count >12,000 or <4000 cu/mm or 10% immature (band) forms 	3	Severe

Table 3-1: The WIfI classification system of foot ulceration

All classification systems categorize the wounds according to depth, presence of ischemia, and presence of infection. Regardless of which classification system is used, it is essential that the system is used consistently across the healthcare team. Careful documentation is also essential.

4 Diabetic Ulcers: Diagnostic and Prognostic Factors

4.1 Clinical Examination

We define the risk patient in line with the definition from the International Working Group on the Diabetic Foot (IWGDF) as ‘a patient with diabetes who does not have an active foot ulcer, but who has peripheral neuropathy, with or without the presence of foot deformity or peripheral artery disease, or a history of foot ulcer(s) or amputation of (a part of) the foot or leg (79, 80).

Diabetic foot diagnosis should include a thorough documentation of medical history, an exact clinical examination and a number of diagnostic tests.

Medical history

Patients recruited in PHOOTONICS project will provide a full medical history. The duration of diabetes, comorbidities, surgical history, history of previous amputation, hospitalization, previous use of antibiotics and medication should be reported in medical records.

Clinical examination

In the PHOOTONICS project all patients will receive clinical examination. The patients’ general condition for signs of toxicity or sepsis will be assessed. Both feet have to be examined at each follow-up visit for active disease such as ulceration or gangrene. The severity of an active infection has to be staged according to the IWGDF/ISDA classification criteria. In patients with PAD the use of WIfI (wound/ischemia/infection) system to stratify amputation risk and revascularization benefit is highly recommended. For a uniform communication among healthcare professionals, the IWGDF (International Working Group for Diabetic Foot) suggests the SINBAD system, which can also be used for audit of outcome of populations (81).

Lesions such as fungal infection, cracks and skin fissures, deformed nails, macerated web spaces, calluses, and deformities such as hammer toes, claw toes, and pes cavus, which increase the risk of ulceration should be taken into consideration (82) (Fig 1). Plantar pressure distribution measurement (pedography) has to be recorded in all PHOOTONICS patients, in order to identify areas at risk of developing an ulcer. At follow up it is important to feel the temperature of the feet with the dorsum of the hand. A cold foot might suggest ischemia, while increased warmth with redness and swelling might suggest inflammation such as acute Charcot foot or cellulitis.

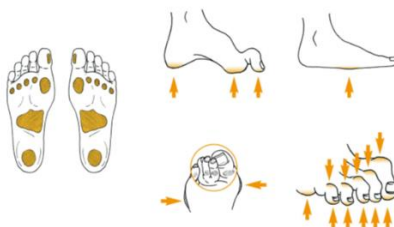


Figure 4-1 Lesions such as fungal infection, cracks and skin fissures, deformed nails, macerated web spaces, calluses, and deformities such as hammer toes, claw toes, and pes cavus, increase the risk of ulceration.

Peripheral artery disease (PAD), generally caused by atherosclerosis, is present in up to 50% of the patients with a diabetic foot ulcer (82). Posterior tibial artery and dorsalis pedis artery in both feet have to be palpated. Absence of pulse must be recorded. The ankle brachial index is an adjunct measure to diagnose peripheral

arterial disease. It is the ratio of the highest systolic blood pressure at the ankle (dorsalis pedis artery or posterior tibial artery) to the systolic blood pressure at the arm and is measured using a Doppler device. It is worth to mention though, that for measuring the ankle brachial index, a Doppler device and elementary training to the procedure are prerequisites. It is obvious that measurement is user dependent. Moreover, people with diabetes can often have falsely raised ankle brachial index levels as a result of poor compressibility of calcified arteries. This will sometimes reduce the informative value of the ankle-brachial index in patients with diabetes (81, 83-86). In such cases, the Toe Brachial Pressure Index (TBPI) and the transcutaneous pressure of oxygen (TcPO₂) may be superior to ABPI measurements. However, TBPI may be influenced by the presence of digital artery calcification. On the other hand, TcPO₂ is time consuming and only feasible selected patients. Therefore, tse two methods are only used in 6.2% and 0.8% of the patients, respectively.

It is obvious that, interpretation of audible Doppler arterial signals using handheld Doppler devices remains the most commonly used bedside test, but this is also limited by significant inter-observer variation and poor sensitivity in detecting PAD (79, 87-89). All clinical centers participating in the PHOOTONICS consortium have vast experience with the diagnosis and treatment of PAD. Hence, we will be able to reliably assess the ankle brachial index in all recruited patients.

Table 4-1 Clinical examination parameters taken into consideration for diabetic foot

CLINICAL EXAMINATION FOR DIABETIC FOOT						
GENERAL CONDITION	FOOT TEMPERATURE	ACTIVE DISEASE	SKIN LESIONS	DEFORMITIES	PAD	NEUROPATHY
Frailty, sarcopenia	Decreased (ischemia)	local cellulitis	fungal infection	hammer toes	tibial pulses	monofilament test
Fever, white blood count	Increased (infection)	ulcer	skin fissures, cracks	claw toes	ankle/brachial index (ABI)	graduated tuning fork
pain		tissue loss	deformed nails	pes cavus	TBPI, TcPO ₂	biothesiometer
toxicity, confusion		osteomyelitis	macerated web spaces, calluses	limited joint mobility		
sepsis		gangrene		plantar pressure measurement		

Uncontrolled diabetes contributes to the development of neuropathy. Diabetic peripheral neuropathy (DPN), a common complication of diabetes, develops at approximately 30% to 50% of diabetes mellitus patients. DPN is crucial to the occurrence and the severity of sarcopenia, and its relationship with muscle weakness has been reported in several studies. Metabolic and microvascular impairments in DPN, affect the intraneural capillaries, which are supplying the peripheral nerves, and result in sensory loss, pain, and muscle weakness. Compared with diabetes alone, DPN can lead to accelerated muscle mass loss in diabetic patients (90).

The aim of screening for diabetic peripheral neuropathy is to identify patients with loss of protective sensation in the feet. Most guidelines recommend the 10 g monofilament for neuropathy assessment in people with diabetes. This monofilament exerts a 10 g buckling force when it bends. Inability to sense a 10 g pressure is the current consensus definition of loss of protective sensation. The test is portable, cheap, and easy to perform. The test may be combined with another test to screen for neuropathy, such as a biothesiometer or a graduated tuning fork (Rydel Seiffer) to assess vibration perception threshold (27, 81, 91, 92). The clinical examination of the diabetic foot has to include all of the aforementioned parameters (Table 4-1).

Follow up

The suggested frequency of follow-up examinations is based on expert consensus (Fig.2) (82). For people at low risk, annual foot assessments are acceptable, unless patients progress to moderate or high risk. More frequent follow-up examinations every 3-6 months should be advised to patients at moderate or high risk such as those with a foot deformity or with a diagnosis of peripheral neuropathy or peripheral arterial disease at initial assessment. Patients with calluses and deformed toe nails requiring preventive podiatry services for basic nail and skin care, debridement of calluses or surgical debridement need a monthly follow-up (65, 93).

Table 1. The IWGDF Risk Stratification System and corresponding foot screening and examination frequency

Category	Ulcer risk	Characteristics	Frequency*
0	Very low	No LOPS and No PAD	Once a year
1	Low	LOPS or PAD	Once every 6-12 months
2	Moderate	LOPS + PAD or LOPS + foot deformity or PAD + foot deformity	Once every 3-6 months
3	High	LOPS or PAD, and one or more of the following: <ul style="list-style-type: none"> ▪ history of a foot ulcer ▪ a lower-extremity amputation (minor or major) ▪ end-stage renal disease 	Once every 1-3 months

Note: LOPS = Loss of protective sensation; PAD = peripheral artery disease. *: Screening frequency is based on expert opinion, since no evidence is available to support these intervals. When the screening interval is close to a regular diabetes check-up, consider to screen the foot at that check-up.

Figure 4-2 The suggested frequency for follow-up based on expert consensus

4.2 Traditional Tests

4.2.1 Diabetic foot and vascular ultrasound

Atherosclerosis is one of the most serious complications of type 2 diabetes. Early onset of atherosclerosis in type 2 diabetes with typical diffuse development in small peripheral vessels leads to increased stiffness of these vessels. Ultrasonographic methods are valuable, non-invasive tools that may be repeated multiple times to assess the stage of the disease and patient's need for treatment, as well as to monitor the results of treatment procedures (80).

The development of atherosclerosis in the course of diabetes consists in the process of vessel wall remodeling. At the early stage of atherosclerosis, remodeling allows for maintenance of the flow lumen as it consists in centrifugal thickening of the vessel wall, with increase in overall vessel diameter (outward

remodeling). In a more advanced stage of atherosclerosis, the wall undergoes inward hypertrophy, leading to stenosis of the flow lumen (inward remodeling). The outward remodeling of the vessel wall is a compensatory mechanism that allows for a non-narrowed flow lumen to be preserved, consisting an early marker of atherosclerotic lesions (94, 95). In addition, clinical presentation of diabetic angiopathy may be altered by calcifications of arterial intima media, that are commonly observed in diabetic patients. The type and stage of vessel wall remodeling in diabetic patients is influenced by numerous factors, including hyperglycemia and hypertension and particularly diabetic dyslipidaemia (96, 97).

Color Doppler imaging of the blood flow is helpful in the assessment of vessel lumen diameter. The enhancement of the color-coded flow signal is selected so as not to exceed the vessel wall. The power Doppler technique is another method that might help in the assessment of the lumen flow; Such possibility is also offered by coded B-flow imaging. B-flow imaging (BFI) is characterized by higher spatial and temporal resolution than Doppler imaging, that allows for a better visualization of the vessel wall. Limitations of the method include turbulence of flow signals in the areas of calcified plaques and calcifications within the vessel walls and limitations in the assessment of the lumen and the wall at high pulsation of the vessel. As in other ultrasound flow assessment methods, the sensitivity of the technique is decreased with depth. B-flow imaging technique is free of typical artifacts such as color blooming or aliasing (98-100).

Duplex sonography (strictly meaning the combination of pulsed Doppler sonography with real time B mode ultrasound imaging, but in current practice usually also including color Doppler scanning) allows the detection of Doppler flow patterns in a precisely defined area within the vessel lumen, facilitating the localization of arterial stenoses. Stenosis is graded by the ratio between the peak systolic velocity of the target/stenosed vessel and adjacent or contralateral non-stenosed vessels: the peak systolic velocity ratio.

Duplex scans of normal lower extremity arteries present the typical triphasic velocity waveform. Heart systole results in the initial high velocity forward flow phase and then, a brief reverse flow phase follows in early diastole. Later in diastole, a final low velocity forward flow appears. Loss of elasticity due to calcification leads to a biphasic or even a monophasic signal, with the absence of early diastolic reversal. Arterial lesions turn the laminar flow into turbulent and cause a widened frequency band (spectral broadening).

Hemodynamically significant stenosis (>50%) is characterized by a peak systolic velocity (PSV) ratio >2. The absence of signal may suggest arterial occlusion. Distal to a significant stenosis, low amplitude systolic signals (monophasic), or continuous antegrade flow appear, or even a tardus-parvus pattern. False positive findings for occlusion may be produced by vessel wall calcification, which is common in diabetics. Infrapopliteal vessel patency assessment is often challenging because of the multiple tandem lesions. Post-stenotic waveforms are indicative of proximal lesions. Vessels that appear occluded in MRangiography, may found to be patent on vascular ultrasound, even with a very low velocity signal (<15cm/s) (101-103).

Unlike MRA, CTA and CA, duplex ultrasound (DUS) does not directly provide the familiar ‘roadmap’ overview of the circulation which facilitates treatment planning. However, the ultrasound operator can draw an informative diagram, particularly helpful in distinguishing the candidates for angioplasty from the patients requiring surgical reconstruction.

A further technical drawback of DUS, which may limit its utility, is the technical difficulty in assessing aortoiliac disease owing to the potential interference by bowel gas and the depth of the vessels. However, the benefits of DUS are that it avoids the possible complications associated with more invasive procedures, it does not involve ionizing radiation or the hazards and contraindications associated with strong magnetic fields, it does also not involve contrast which may cause nephropathy or allergic reactions, and it is relatively

cheap and mobile (104).

Therefore, duplex ultrasound is currently indicated as the first line imaging method to confirm lower extremity artery disease lesions. The Bollinger score is a valid tool used to determine overall lower limb atherosclerotic burden. Its use in randomized trials, primarily as a marker of arterial run-off following bypass surgery, also identified its role as a potential measure of cardiovascular risk. The infra-inguinal arteries are divided into 11 segments to assess the distribution of disease. Each arterial segment is then individually scored for burden of disease, based on the type of lesion (occlusion, stenosis <75%, stenosis <50%, or plaque < 25%) and its extent within the arterial segment (single lesion, multiple lesions affecting less than half of the segment or multiple lesions affecting more than half of the segment). For further analysis, the total Bollinger score is analyzed and the lower limb arterial tree is divided into two groups: the femoral-popliteal (FP) arteries and the crural (CR) arteries. The FP group consists of both the proximal and distal SFA segment, as well as the proximal and distal popliteal artery segments (four segments total). The CR group comprises the tibioperoneal trunk and the proximal and distal segments of the anterior tibial, posterior tibial, and peroneal arteries (seven segments total). An average score per segment is then determined for each of the FP and CR groups. This is calculated by determining a cumulative score for each group and then dividing this by the number of segments actually visualized and scored in that group (105-108).

In PHOOTONICS clinical study the Bollinger score will not be calculated. All participants will be submitted to color duplex ultrasound at enrollment. Stenoses of the femoral and tibial arteries will be assessed by the standard vascular laboratory criteria.

Bollinger Scoring Matrix				
	Plaques < 25%	Stenosis 25 - 49%	Stenosis > 50%	Occlusion
Single Lesion	1	2	4	-
Multiple Lesions Affecting < 1/2	2	3	5	13
Multiple Lesions affecting > 1/2	3	4	6	15

This is used to assess severity of disease in an arterial segment. For each column representing a different disease extent category, only one disease severity can be present (single, multiple lesions affecting < 1/2 or multiple lesions affecting > 1/2 of the arterial segment). Minimum score is 0, maximum score is 15

Figure 4-3 Vascular laboratory criteria of peripheral artery stenosis [Error! Reference source not found.]

Instrumentation

Vascular ultrasound tests require a machine equipped with 5- to 12-MHz linear-array transducers (for extremities) and 2.25- to 3.5-MHz curved linear- or phased-array transducers (for the abdomen). A vascular software package is required in addition to the appropriate transducers. Duplex scanning refers to an ultrasound scanning procedure recording both gray scale and Doppler information. This includes 2-dimensional structure and motion, Doppler spectrum analysis, and color flow velocity mapping.

Principles

The ultrasound beam is directed perpendicular to the surface of interest to obtain the brightest echo with gray-scale imaging and optimal imaging of the artery wall.

Color Doppler

The pulse repetition frequency scale determines the degree of color saturation and is adjusted so that normal laminar flow appears as a region of homogeneous color. Stenosis results in the production of a high velocity jet and an abrupt change in the color flow pattern.

This is identified as either aliasing or desaturation (whitening) of the color display at the site of luminal

narrowing. Color aliasing, persistence, and bruit all indicate flow disturbance.

Spectral Doppler waveform analysis

A normal pulsed wave Doppler waveform is a sharply defined tracing with a narrow Doppler spectrum indicating that blood cells are moving at similar speed throughout the cardiac cycle. Flow becomes turbulent at bifurcations and luminal narrowing causing spectral broadening of Doppler waveform, with filling in of the low velocity region in the spectral waveform as the blood cells move at a wide range of velocities. The normal peripheral artery waveform is triphasic. This diastolic component is absent in stiff atherosclerotic vessels.

Power Doppler

Power (or energy) Doppler is a technique that displays the total strength (amplitude) of the returning Doppler signal without distinguishing direction. Power Doppler can, therefore, identify very slow flow that may not be detected by color flow Doppler. Power Doppler is used to differentiate high-grade stenosis from occlusion, to detect collateral vessels, and to identify small vessel disease

Assessment of arterial stenosis

Doppler velocity is the main tool used to evaluate stenosis severity. Characteristic duplex ultrasound features of stenosis include elevated velocities, color disturbance, spectral broadening, and post-stenotic waveforms. If no post-stenotic turbulence can be identified, inappropriate angle alignment or a tortuous vessel should be suggested as a cause of artifact high velocities.

Interpretation

Peripheral arterial stenosis is characterized using pulsed wave Doppler evaluation. The diagnostic criteria use step-up in PSV ratios from proximal to distal artery and careful waveform analysis. Pulsed Doppler signal at the level of a stenosis reveals a PSV double that of the velocity in the proximal segment. There is spectral broadening and forward flow throughout the cardiac cycle in severe stenosis. An occlusion is present when there is no flow within an arterial segment. High-resistance waveforms are present in the artery proximal to the occlusion if there are no collateral vessels. Continuous forward diastolic flow is present in the proximal artery if dilated high capacitance collaterals are present. The artery that reconstitutes distal to a high-grade stenosis will have a characteristic poststenotic parvus-tardus waveform (109).

192 M Gerhard-Herman et al

Table 15 Diagnostic criteria for peripheral arterial diameter reduction.

	Diameter reduction	Waveform	Special broadcasting	PSV distal/PSV proximal
Normal	0	Triphasic	Absent	+++ No change
Mild	1%–19%	Triphasic	Present	<2:1
Moderate	20%–49%	Biphasic	Present	<2:1
Severe	50%–99%	Monophasic	Present	>2:1*

PSV, Peak systolic velocity.

* > 4:1 suggests >75% stenosis, >7:1 suggests > 90% stenosis.

Figure 4-4 MRA compared to contrast angiography is a less invasive imaging technique.

Doppler examination can accurately diagnose peripheral arterial disease. Compared with the gold standard of arteriography, duplex Doppler evaluation used to detect significant stenoses in patients with proximal lower extremity arterial disease demonstrates a high sensitivity (82%) and specificity (92%). Use of color and pulsed wave Doppler increases the sensitivity (87%–88%) and specificity (95%–99%) of stenosis

identification. The PSV ratio between the stenosis and the immediately proximal artery segment classifies peripheral arterial stenosis better than absolute PSV measurements. For example, PSV ratios of 2 and 7 correspond to stenoses greater than 50% and greater than 90%, respectively. There is a wide range of PSV measurements obtained in the lower extremities of normal and abnormal cases. There is a greater correlation between PSV ratio and stenosis than between absolute PSV and stenosis.

Diabetic foot and contrast angiography, computed tomography angiography, magnetic resonance angiography

Significant progress in limb salvage for diabetic patients with peripheral arterial disease and critical limb ischemia has occurred in the past decades. Improved diabetic patient outcomes are due to accumulated information on the disease processes and to the beneficiary results of revascularization techniques.

A non-invasive, reliable, user friendly imaging modality would be a useful tool for clinicians in assessing lower-extremity perfusion when planning interventions. In an effort to achieve this goal, emerging regional perfusion imaging modalities are transcutaneous oxygen monitoring, hyperspectral imaging, indocyanine green dye-based fluorescent angiography, nuclear diagnostic imaging, and laser Doppler. Nevertheless, traditional contrast angiography, computed and magnetic angiography remain the most widely performed imaging techniques. All of the tests aim to determine regional foot perfusion and, possibly, guide directed revascularization therapy in patients with critical limb ischemia and foot ulceration. There are differences in availability, cost, operator dependence and diagnostic accuracy (Table 4-2). Therefore, for each patient the indicated diagnostic protocol has to be followed according the existing guidelines (110).

Table 4-2 Availability, cost, operator expertise, diagnostic accuracy for DSA, CTA, MRA in LEAD diagnosis

Imaging method	DUS	CTA	MRA	DSA
Availability	+++	++	++	+++
Costs	+	++	+++	+++
Operator expertise	+++	+	++	++
Diagnostic accuracy				
Aorto-iliac	++	+++	+++	+++
Femoropopliteal	+++	+++	+++	+++
Tibial	+	+	++	+++

Contrast angiography

Digital subtraction angiography (DSA) is a fluoroscopy technique, performed in interventional radiology departments. The technique provides blood vessels visualization in a bony or dense soft tissue environment. Images are created by injecting contrast medium intra-arterially, while subtracting, in the same time, a "pre-contrast image" or *mask* from subsequent images. Subtraction angiography was first described in 1935 as a manual technique. Digital technology was introduced in the 1970s and made DSA the gold standard of

vascular imaging.

In traditional angiography, images are obtained by exposing a part of the patient's body to time-controlled x-rays, while injecting contrast medium into arteries that are going through the area of interest. In the provided image, blood vessels, along with all the overlying and underlying structures are depicted. These images are useful for determination of anatomical position and variations, although dense structures prevent us from visualizing blood vessels accurately.

In order to bypass the overlying structures and clearly see the vessels, first a mask image is acquired. The mask image is the image of the area of interest, before the contrast is administered. The radiological equipment required to proceed this subtraction is a properly designed X-ray image intensifier, capable of producing images of the same area at a set rate (1 to 7.5 frames per second) and then, store them. Each subsequent image gets the original "mask" image subtracted out. The images are all produced in real time by the computer or image processor, while the contrast is injected into the blood vessels (111, 112). Intra-arterial contrast angiography is considered to be the reference standard. The main disadvantages are those associated with arterial puncture, ionizing radiation, allergic reactions and potential nephrotoxicity of iodinated contrast agents.

Several alternative imaging techniques are available, including magnetic resonance angiography, computed tomography angiography and duplex ultrasonography. These techniques are less invasive than contrast angiography, although computed tomography angiography carries risks relating to ionizing radiation, and both contrasts enhanced magnetic resonance angiography and computed tomography angiography carry risks associated with the use of contrast agents.

Because of its lack of nephrotoxicity or atopic reactivity, CO₂ has been proposed as a reliable alternative to iodine-based contrast agents in peripheral angiography of diabetic patients, especially when the renal function is impaired. CO₂ is less viscous than iodine-based contrast material. Moreover, it does not dilute, resulting in a better filling of distal vessels in the case of proximal occlusion. Automated Carbon Dioxide Angiography (ACDA) is an accurate, safe, and effective technique that can be performed to guide endovascular interventions in diabetics with CLI and baseline CKD (Chronic Kidney Disease) (113).

Magnetic resonance angiography

With DSA technique, detailed description of the calf vessels may not be successful when multiple stenoses are present. Several studies have demonstrated that accurate delineation of runoff vessels in diabetic patients with peripheral artery disease is not feasible with DSA. MR angiography is a modern technique with promising results in diabetic PAD. High spatial resolution is necessary because of the distal location of the arterial stenosis. In addition, high temporal resolution is required to eliminate the interference of the venous signal.

Magnetic resonance angiography (MRA), compared to contrast angiography, is a less invasive imaging technique (Figure 4-5). Both time-of-flight (TOF) and phase-contrast (PC) MRA are non-contrast techniques with intravascular blood detection based on flow properties, as opposed to standard position of the surrounding tissues. Contrast-enhanced (CE) MRA is based on the T₁ shortening effect of intravenously administered contrast media. TOF techniques use gradient echo pulse sequences in which protons entering the frame (such as those in flowing blood) are unsaturated compared with static ones and so emit a higher signal, the latter being the basis of the contrast. Compared with the two-dimensional (2D) method, three-dimensional (3D) TOF provides a higher signal-to-noise ratio and shorter imaging times; however, it is more susceptible to saturation effects. Phase-contrast methods are based on phase shifts transmitted by protons going through a gradient magnetic field, whereas stationary protons present no phase change. Technical

drawbacks with the use of TOF and PC MRA in PAD include motion artifacts, long acquisition times, low spatial resolution, unreliable delineation of lesions with high flow and turbulence (major signal loss at regions of high grade stenosis), and failure to detect any patent vessels with reversed blood flow. Further considerations for the MR studies are the exclusion or appropriate management of patients with pacemakers or some other metallic implants and joints, along with the patients suffering from claustrophobia.

Some of the aforementioned technical implications have been discarded by contrast-enhanced techniques, the most commonly used MRA method for assessment of PAD. CE MRA is flow independent, therefore most of the artifacts due to flow turbulence and low-flow that are problematic in TOF and PC MRA, are set aside. With CE MRA, acquisition times are reduced, and the quality of images is improved. Moreover, with flow independence, in-plane imaging of vessels is achieved, and the number of image slices needed to cover an extended vascular territory is diminished. Therefore, faster high-resolution imaging is possible. In



Figure 4-5 MRA and CTA roadmap for the same patient

combination with a moving table this allows the whole of the lower limb vascular tree to be covered in three steps after a single contrast injection. CE MRA may also highlight patent distal segments that are not discrete with TOF techniques or CA. Additional disadvantages of the CE MRA technique is allergic reaction and the long-term nephrotoxicity of the magnetic contrasts. Arterial puncture and the relative complications are excluded, due to intravenous magnetic contrast administration.

Recent studies suggest the superiority of contrast-enhanced MR angiography over DSA for the identification of patent arterial segments in runoff vessels of the foot in both diabetic and nondiabetic patients. Dorweiler et al. (114) showed that foot vessels that were not seen on conventional angiography but were detected on MR angiography were patent target vessels for pedal bypass grafting. This advantage of MR angiography particularly clear in infrapopliteal vessels may be explained by several reasons: MR angiography can trace blood flow at velocities as low as 2 cm/sec, whereas in DSA, the dilution of contrast medium beyond long-occluded segments doesn't allow for sufficient enhancement of distal vessels. The ACC/AHA guidelines support the use of CEMRA of the extremities to diagnose the anatomic location and degree of stenosis of PAD (level of evidence: A) and recommend that MRA should be performed with gadolinium enhancement (level of evidence: B), underlining its value in selecting patients with lower extremity PAD, suitable for endovascular intervention (level of evidence: A). The use of CEMRA studies requires double dose (0.2 mmol/kg) IV contrast administration, often placing diabetic patients with renal impairment at high risk for nephrogenic systemic fibrosis (NSF). Therefore, both dosage options and the ability to repeat non-diagnostic studies are restricted.

No single technique for peripheral MR angiography has been universally accepted. Some authors have supported peripheral MR angiography with multiple stacks. However, this technique has not gained widespread clinical acceptance, as for imaging of the entire vascular tree, both repeated placement of the patient in the scanner and repeated injections of contrast media are required. Unfortunately, by this way the examination is time-consuming. Moreover, a poor contrast-to-noise ratio is produced after the first stack because of the increased contrast enhancement of surrounding tissue. Another drawback is the low accuracy of arterial analysis by venous overlay. The three-station technique using a moving bed was introduced to overcome these limitations.

A hybrid MR angiography protocol, focusing separately on pelvis-to-thigh arteries and on calf and dorsalis pedis arteries, was recently described with promising results. This is a reliable method for investigating PAD in selected diabetic patients with critical limb ischemia. Moreover, lower extremity vessels invisible with conventional angiography can be detected. The technique avoids iodinated contrast material-induced renal

failure and may be useful for treatment planning in this setting. Although many considerations of the previous MR techniques have been overcome with the hybrid MR angiography, there are still a few disadvantages. First, the hybrid MRA protocol requires a 60- to 90-min interruption, a fact that makes the procedure impractical. Another potential limitation for its widespread clinical use may be the high rate of contraindications. Patients with intraarterial stents, suitable to MR angiography, have to be excluded from hybrid MRA protocol. Signal loss in the stent impairs the analysis of the vessel lumen and this impairment may potentially bias the study (114-123).

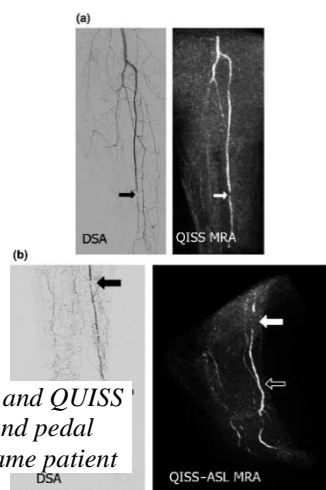


Figure 4-6 DSA and QUISS MRA for tibial and pedal arteries of the same patient

The high prevalence of chronic renal impairment in diabetic patients with PAD and the need for high doses of gadolinium-based contrast agents impose the risk for nephrogenic systemic fibrosis. The need of unenhanced MRA techniques for the assessment of symptomatic PAD is obvious. Such techniques are the gated 2D time of flight, the 3D phase contrast and subtractive techniques (fresh blood imaging, native spatial and chemical-shift-encoded excitation (SPACE), and flow-sensitive dephasing). Each of the aforementioned unenhanced MRA methods has advantages and drawbacks.

Compared with subtractive techniques, quiescent-interval single-shot (QUISS) MRA is fast, motion insensitive, and does not require patient-dependent adjustments. The QUISS MRA technique is capable of imaging over a vascular territory more than 1 m long in a short scan time, taking into consideration the large velocity variations among vascular segments. Furthermore, patients with PAD often suffer from coexistent cardiac disease and resultant arrhythmias which may produce artifacts in MRA examination. In addition, respiratory motion may complicate the imaging of the abdomen and pelvis. The QUISS technique addresses all of these challenges. Scan times to cover a region from the renal arteries to the feet are usually less than 7 minutes. In most cases, neither variations in flow velocity nor arrhythmias produce substantial alterations in vascular signal intensity. Because data for each slice are acquired during a single shot of only a few hundred milliseconds, QUISS is naturally motion resistant. Respiratory motion can be further smoothed through the use of breath-holding or signal averaging. Unenhanced MRA technique is feasible to assess vascular status in diabetic patients with symptomatic PAD and that this technique is a valuable tool in this setting. With the QUISS unenhanced MRA sequence, imaging of the vascular tree from the infrarenal aorta to the pedal vessels can be achieved before contrast injection. This method is particularly useful in patients with advanced PAD, lower limb diabetic ulceration, or other risk factors for a non-diagnostic CEM-RA runoff (Figure 4-6).

QUISS unenhanced MRA can be particularly useful for the evaluation of PAD in patients with impaired renal function or other contraindications to contrast administration. In addition, it could provide a reliable alternative to other, invasive or noninvasive examinations, especially for diabetic patients who have heavily calcified peripheral arteries. Besides, the accuracy of MRA is not expected to decrease by the presence of calcifications (124-128).

Recently, additional improvements of MR angiography have been described. Partially, parallel acquisition imaging claims to offer faster acquisition and will probably find many applications in MR angiography in the future. With the improvements in high gradient technology and the use of evolved vascular contrast mediums, the accuracy of MR angiography is likely to improve.

Computed tomography angiography

Recently, MDCT (multidetector computed tomography) angiography was introduced for the evaluation of

peripheral vascular disease. Progress in multidetector technology improves the speed of acquisition and provides high spatial resolution. The modern multidetector row machines have enabled fine collimation to be combined with rapid (arterial phase) contrast enhanced scanning. Therefore, imaging of the extended length of the lower limb vascular tree, from suprarenal aorta to the ankles, is possible with a single helical acquisition (Figure 4-7).

Although CTA avoids the potential complications associated with arterial puncture, in common with CA it still requires exposure to ionizing radiation and the injection of relatively large volumes of iodinating contrast material. Allergic reactions and contrast related renal failure is some of the drawbacks of the technique. In addition, in cases of severe diffuse calcification, particularly of the small calf or ankle vessels, the accuracy of the method is diminished. Besides, CTA presents lower resolution compared to digital subtraction angiography. This is of particular interest for diabetic patients who present heavier below the knee arterial calcification, compared to patients without diabetes mellitus (129).



Figure 4-7 CTA road map, 3-D technique

It is worthwhile to mention that CT technology has been rapidly progressing both in terms of hardware and software. Dynamic CT is an additional method, introduced to overcome the drawbacks of conventional CTA in evaluating smaller arteries below-the-knee arteries. The increased radiation dose, along with the increased amount of necessary iodinated contrast medium is the disadvantages of the technique. These limitations will be overcome if scan intervals and contrast medium injection protocols are optimized.

Selective dual-energy reconstruction and dynamic CT are alternative promising techniques, aiming to overcome the disadvantages of CTA in the visualization of calcified small arteries of the lower limb. Intra-arterial dual energy CTA allows for accurate and detailed preoperative imaging of the infrapopliteal arteries.

Even with the most recent CT technology, the evaluation of smaller arteries, particularly those with diameters <3 mm and arterial wall calcifications or metallic stents, has remained challenging and time-consuming. Recently, an ultra-high-resolution CT (UHRCT) system has been introduced, which increases spatial resolution more than twofold. The improved spatial resolution may particularly serve in imaging of the small vessels. In combination with post-processing advances (subtraction technique), these developments may overcome some of the current limitations. More detailed, non-invasive diagnosis of PAOD will be therefore available.

The 0.25-mm effective size of the detector element on UHRCT enables the visualization of smaller structures more precisely. The images are approaching the reference standard of DSA, yet with better opacification in certain cases. Another use of UHRCT is the non-invasive visualization of the collateral arteries, pedal arch, and digital arteries. Evaluation of distal smaller arteries is very important in patients with severe limb ischaemia. The status of distal run-off is thought to be an important predictor of remote patency of the bypass graft or re-canalised proximal artery. In addition, poor collaterals and severe stenosis at the level of the pedal arteries might lead to considerable tissue limitations that should be addressed. First, acquiring thinner sections without changing the signal-to-noise ratio can result in higher radiation doses despite the use of a hybrid iterative reconstruction. A full iterative reconstruction method could be highly beneficial in this scenario even if the proximal lesions are successfully treated.

UHRCT using subtraction technique has the potential for visualizing small vascular structures and may improve our understanding of the distal run-off status especially in severe limb ischaemia. The angiosome concept is also becoming important. The evaluation of tissue perfusion and distinction between hyperemia and congestion in damaged areas could also become important markers for avoiding major tissue loss (130-

137).

Run-off Computed Tomography Angiography (run-off CTA) of the lower extremities has recently evolved by the addition of time-resolved CT scan series, with performing of repeated axial acquisitions over the calves of the patient during a second bolus of iodinated contrast injection (138).

Advantages and disadvantages of the imaging techniques for diabetic peripheral angiopathy, along with accuracy and indication parameters are presented in Table 4-3.

Table 4-3 Comparison of different imaging tests for patients with LEAD

	DSA	DUS	CTA	MRA
Advantages	<ul style="list-style-type: none"> • Delineation of the vessel lumen • Roadmap (scanning of the entire vascular tree) • Gold standard 	<ul style="list-style-type: none"> • Noninvasive/ bedside technique • Non-radiating/lack of complications • Wide availability • Low cost • Anatomic and hemodynamic data 	<ul style="list-style-type: none"> • Noninvasive • Rapid • Roadmap • Lumen, wall (calcifications) and extraluminal information • Visualization of stents, bypasses, aneurysms • 3-D reformatting 	<ul style="list-style-type: none"> • Noninvasive • Non-radiating • Anatomic and functional information • Independent of calcifications
Disadvantages	<ul style="list-style-type: none"> • Invasive • Radiation • Contrast nephrotoxicity • Contrast anaphylactic reactions 	<ul style="list-style-type: none"> • Operator-dependent • Poor visualization of heavy calcified vessels/poor discrimination of high grade stenosis-total occlusion • Poor visualization of iliac vessels if obesity/bowel gas • No clear roadmap 	<ul style="list-style-type: none"> • Contrast nephrotoxicity/ anaphylactic reactions • High radiation dose • Lack of hemodynamic data • Cost • Limited availability • Stenosis overestimation (distal arteries) 	<ul style="list-style-type: none"> • Cost • Limited availability • Time consuming/ motion artifact vulnerability • Overestimation of stenosis • Gadolinium induced nephrogenic systemic fibrosis • Claustrophobia • Incompatibility with pacemakers • Poor visualization of stents • Limitations of selection of anastomosis site for a bypass
Sensitivity		85-90%	Aortoiliac 96% Fem/pop 97%	95%
Specificity		>95%	Aortoiliac 98% Fem/pop 94%	95%
Best practice	<ul style="list-style-type: none"> • Discordant non-invasive imaging results • Below knee lesions in critical ischemia • In combination with endovascular intervention 	<ul style="list-style-type: none"> • LEAD detection • Follow up of treatment • Venous graft suitability assessment 	<ul style="list-style-type: none"> • Aortoiliac lesions • Aneurysms • Extravascular pathology • Stent/bypass assessment • Planned intervention for revascularization 	<ul style="list-style-type: none"> • Planned intervention for revascularization • Patients with moderated renal failure • Inconclusive DUS results

4.2.2 PHOOTONICS diagnostic imaging protocol

For the management of PAD of the lower extremities, guidelines have been released by the following organizations:

- American College of Cardiology/American Heart Association (ACC/AHA)
- Society for Vascular Surgery (SVS)
- European Society of Cardiology (ESC)
- ESC/European Society for Vascular Surgery (ESVS)
- SVS, ESVS, and World Federation of Vascular Societies

For symptomatic patients who may be candidates for revascularization, the ACC/AHA and SVS guidelines recommend imaging studies such as duplex ultrasound (DUS), computed tomography angiography (CTA), magnetic resonance angiography (MRA), and contrast arteriography. The use of segmental pressures and pulse volume recordings to assess localization and severity are alternative diagnostic techniques.

The ESC/ESVS propose DUS as a first-line imaging method to confirm lower extremity artery disease (LEAD). DUS and/or CTA and/or MRA are indicated for anatomic characterization of LEAD lesions and guidance for optimal revascularization strategy. Data from anatomic imaging tests should always be combined with symptoms and hemodynamic tests prior to a treatment decision (139-142). In PHOOTONIC project, all recruited patients will be submitted to DUS. Patients with diabetic ischemic ulcers who are candidates for intervention or when DUS findings are inconclusive, will be submitted to either DSA or MRA or CTA, according to the aforementioned guidelines.

4.3 Complementary tests

Complementary tests for diabetic foot.

Between 20–50% of patients being diabetic for more than 10 years, will present symmetric distal sensory neuropathy, leading to a progressive, distal to proximal, loss of sensation (temperature, pain) in the lower extremities. Local foot paresthesias and lack of sensation over foot pressure points result in multiple painless microtrauma, insidious breakdown of overlying tissue, and eventual ulceration. Typically, DPN affects the sensory nerves. However, DPN can also affect the motor nerves that are responsible for the function of muscles. Damage to motor nerves can cause muscle wasting, along with a loss of motor balance of flexor and extensor muscles. This process alters the normal structure of the foot and creates deformities, such as claw toes or prominent metatarsal heads. Consequently, additional pressure points prone to ulceration are formed. Abnormal pressure distribution (APD) can be detected as the first pathology, often preceding the visible abnormality.

In the PHOOTONICS project, nerve conduction studies and plantar pressure measurement have to be included in the diagnostic protocol.

Nerve conduction studies (143)

Worldwide, DPN is defined as “the presence of symptoms and/or signs of peripheral nerve dysfunction in people with diabetes, after the exclusion of other causes”.

The progression of neuropathy has proved to be continuous, from normal nerve function to subclinical

neuropathy, that can be detected with electrophysiological tests, to final overt neuropathy, clinically diagnosed. In symptomatic diabetic neuropathy, there is slowing of nerve conduction velocity, owing to demyelination and loss of large myelinated fibers. Additionally, the nerve action potentials are reduced as a result of axons loss.

The pathogenesis of DPN is multifactorial. Patient's susceptibility, vascular, metabolic, and environmental factors contribute to DPN pathogenesis. Different causative mechanisms have been implicated: irregular polyol and myo inositol metabolism, reduction of Na/K-ATPase, intraneural microvascular impairment with subsequent ischemia, toxic effect of oxygen radicals, neurotrophic deficit (IGF-I, NGF), defective axonal transport and non-enzymatic glycosylation of neuronal structural and transport proteins. The main risk factors for DPN are the poor glycemic control, long duration of diabetes, older age of onset, male gender, height, alcohol use, hypertension, nicotine use, and hyperlipidemia.

Sensation loss in the beginning is usually peripheral, sock-like, and symmetrical. Achilles reflex and, sometimes, patellar reflex are also reduced. Muscular dysfunction often presents with atrophy of the anterior muscle group of lower leg and malposition of toes. Moreover, during the rollover process of gait, the forefoot pressure is increased and abnormally distributed.

The main drawback of NCS is that small myelinated and unmyelinated nerve fibers, which are affected early in the disease course of DPN, do not contribute to the sensory action potential detected by routine NCS. The sensory action potential is altered only after involvement of larger myelinated fibers, which is often a late event in patients with diabetes. Electrophysiological data must, therefore, always be evaluated in the clinical context.

Nerve Conducting Studies (NCS) have to be performed in all patients recruited in PHOOTONICS project. The results of the tests must be interpreted with respect to clinical data.

Plantar pressure measurement (4, 144-146)

Measurement of the plantar pressure, i.e. the distribution of force over the sole of the diabetic foot, is useful as it provides detailed information specific to each region of contact. The physiological pressure distribution pattern on the plantar surface is nearly symmetric and assures the optimal stabilization of the body. Normally, there are three main points of the highest load on the plantar surface: the central part of the heel, along with the 1st and 4th-5th metatarsal heads. In diabetic patients, the sole loading pattern is altered. The region with the higher plantar pressure is the central metatarsal heads (II-IV metatarsophalangeal joints), where foot ulcers usually occur. In the Eurodiale study, about 55% of diabetic ulcers were located on patients' toes but 22% of all ulcers affected the forefoot/midfoot area.

Different activity profiles, when patients are turning, shuffling, climbing stairs, or simply standing, provide various patterns of plantar pressure magnitude and distribution. A unique plantar pressure threshold for foot ulceration has not been confirmed from medical studies, as false-positive and false-negative results may occur. Shear stress is also considered important in foot ulcer development, but has received little attention so far.

A wide variety of measurement systems are available on the market. In general, these can be distinguished according to different sensor principles (resistive, capacitive, piezoelectric) and different devices (platform, insole, single transducer system). Platform systems have the limitation to be used in a laboratory setting (embedded in a walkway) and only for barefoot measurements. Insole or single transducer systems can be used to detect the plantar pressures within the shoe and therefore are appropriate to assess the effects of different shoe configurations.

Platform systems include a flat, rigid array of pressure sensing elements arranged in a matrix configuration, incorporated to the floor to allow normal gait. Platform systems can be used for both static and dynamic studies

In-shoe sensors are flexible and embedded in the shoe in a manner that reflects the interface relation between the foot and the shoe. The system is portable.

For real-time measurement of natural gait parameters, sensors should be mobile, untethered, and able to be placed in the shoe sole and to sample effectively in the target environment.

In designing plantar pressure measurement devices the key requirements are spatial resolution, sampling frequency, accuracy, sensitivity, and calibration. In order to be mobile and wearable for monitoring activities of daily life, the system should be light, wireless, portable, inexpensive, with low power consumption and with the potential application to data transfer communication systems.

5 Photonics Based Diagnostic Tests

Spectroscopy involves the study of objects based on their wavelengths when they are emitting as well as absorbing light. Infrared (IR) and near-infrared (NIR) regions of the electromagnetic spectrum have been mostly used for non-invasive methods of diabetic foot ulcer (DFU) detection. Hyperspectral imaging (HSI) is a technique combining spectroscopy and imaging, where each image is acquired at a narrow band of the electromagnetic spectrum. Hyperspectral imaging divides the spectrum in bands, typically covering the visible and near-infrared range. Thermal imaging is simply the process of converting infrared radiation (heat) into visible images that depict the spatial distribution of temperature differences in a scene viewed by a thermal camera. Hyperspectral and thermal imaging can be valuable technologies in the prevention and management of diabetic foot disease; thus, they have been widely used in clinical practice. In addition, technological advancements in these imaging technologies increase their application range. Here, we collect the existing medical studies and clinical trials on how hyperspectral imaging and thermal imaging can improve the diagnosis, monitoring and management of DFUs and under which medical conditions. Temporal changes in local epidermal thickness and oxyhemoglobin concentration are factors of great interest for diabetic foot ulcer monitoring (147). Due to the different absorption spectra of oxy and deoxyhemoglobin, hyperspectral imaging has been utilized to capture the various reflectance spectra and estimate oxygen saturation (SpO₂) values from peripheral tissue (148). On the other hand, thermal imaging is also a promising technology to achieve this objective, as increased plantar foot temperature is a key sign of underlying inflammation. Infrared images are useful for measuring temperature in foot surface and for detecting temperature differences (>2.2 °C) between a foot region and the same region on the contralateral foot [**Error! Reference source not found.**]. In particular, we gather all the good practices, the summary outcomes and lessons learned from the existing literature in terms of (a) medical indices use (e.g., temperature, hemoglobin, oxyhemoglobin and deoxyhemoglobin), (b) the value ranges of these indices for the healthy and non-healthy tissues, (c) how parameters such as gender and age can affect the value ranges and discrimination resolution, and other criteria (excluding, percentage of correlation of the medical indices with the disease and its progress), in order to come up with an efficient solution and processing strategy for the PHOOTONICS project. For this reason, the literature is divided in two main categories, in order to ensure a proper comparison among them, based on type of medical imaging used: (a) studies that make use of infrared thermal images, and (b) studies that use hyperspectral imaging technologies.

Except for temperature distribution in DF and concentration in oxyhemoglobin and deoxyhemoglobin, spectroscopic techniques have been used for non-invasive methods of blood glucose measurement, mostly including near-infrared spectroscopy, Raman spectroscopy, bio-impedance spectroscopy, and thermal emission spectroscopy. NIR uses infrared to capture reflected light from body tissue, indicating a level of blood glucose, while thermal emission spectroscopy measures IR signs produced in the body as a result of glucose concentration changes (149).



Figure 5-1 Example of thermal imaging [**Error! Reference source not found.**]

5.1 Thermal imaging and Long IR spectrum

5.1.1 Medical Infra-Red Imaging Fundamentals

Infrared thermography (IRT) is a fast, passive, non-contact and non-invasive alternative to conventional clinical thermometers for monitoring temperature in parts of the human body. The first modern infrared detector was originally developed for military applications, around World War II, and later, the technology was released for civilian use. In IRT, thermal patterns on the surface of the test objects are monitored. Subsurface defects cause abnormal thermal patterns, which indicate the presence of those defects. Similarly, in medical applications, due to clinical illness abnormal thermal patterns on the skin surfaces are monitored. Since multiple disease patterns can be diagnosed through information on the body's temperature distribution, thermography represents a highly flexible procedure, which is, in comparison to other processes in medical engineering, budget-friendly (150).

A thermal imaging camera consists of five components: an optic system, detector, amplifier, signal processing, and display. MIT (Medical Infrared Thermography) is essentially a digital two-dimensional imaging technique that provides data about the physiology of tissues. Unlike most diagnostic modalities, MIT is non-invasive.

An infrared camera suitable for evaluating human skin profiles should have the following:

- *High Spatial resolution* which reflects the separation between two nearby spots. A resolution of 320 (horizontal) × 240 (vertical) pixel is the minimum requirement. The spatial resolution is very dependent on image focusing.
- *High Thermal resolution* as an expression of sensitivity, defined as the minimum temperature difference that can be measured at two distinct spots.
- *Medical CE certification* is recommended: As soon as a temperature value in degree celcius is stated, the device is classified as a medical modality with a measuring function and should be signed by a specific CE approval.
- *Narrow Calibration range* accustomed to the human temperature range (*i.e.*, 20–40 °C) assures more detailed temperature readings.

5.1.2 Medical Infra-Red Images for diabetic foot ulceration

Infrared cameras are increasingly applied in clinical applications as they allow fast, inexpensive and non-contact temperature measurements. As abnormal heat distribution can indicate illness, infrared cameras have been applied in the prediction, diagnosis and monitoring of diabetic foot ulcer. Infrared thermography, which has been considered as a non-invasive diagnostic tool since 2001, is a technique used in studies of prevention and evaluation of Diabetic Foot (DF). In this section, a summary table (Table 5-1) that presents the published works related to DF diagnosis and infrared thermography follows. The comparison is conducted in four basic categories for each research:

- the equipment used (cameras, thermometers, etc.), as well as the environment conditions of the experiment,
- the number of participants and their characteristics (age, gender, etc.),
- the processing strategy that each research follows,
- the results.

Then, a brief outcome follows, with some conclusions and proposed solutions regarding the good practices and optimal characteristics that we should take into consideration in our case.

Table 5-1 Summary of Literature: Review Table of the Published Works Related to DF Diagnosis with Infrared

Thermography

A / A	Reference	Basic Equipment and Environmental Conditions	Participants (Number and characteristics)	Image analysis Processing Strategy	Experimental Results
1	Van Netten et al., 2013 (148)	<ul style="list-style-type: none"> RGB camera, <i>Canon Eos 40D with EF-s 17–85 mm lens</i>, IR Thermal camera, <i>FLIR SC305 with 16 bit resolution</i> 	15 diabetes patients	Analyze Mean temperature difference by the Kruskal–Wallis tests.	Average Temperature in regions of interest (ROIs), Standard deviation (SD). Patients (criteria > 2.2.°C): <ul style="list-style-type: none"> without complications showed small temperature differences between feet (ΔT). with local complications such as a noninfected and nonischemic foot ulcer showed $\Delta T > 2$ °C. with diffuse complications such as a foot ulcer with osteomyelitis or a Charcot foot showed $\Delta T > 3$ °C.
2	Liu et al., 2015 (151)	<ul style="list-style-type: none"> commercial digital RGB camera, <i>Canon EOS 40D</i> IR camera, <i>FLIR SC305</i> 	76 diabetes patients (7 patients with type I DM and 69 patients with type II DM)	Asymmetric analysis (K-means clustering, EM Algorithm for Foot segmentation, registration and detection)	Temperature differences between contralateral points, Average, SD. Foot segmentation in the thermal images achieve accuracy 97.9% +/-1.1% and 98.3% +/- 0.5%.
3	Petrova et al., 2018 (152)	thermal imaging device (Diabetic Foot Ulcer Prevention System (DFUPS), constructed by Photometrix Imaging Ltd) and also with a hand-held infrared spot thermometer (Thermofocus® 01500A3, Tecnimed, Italy)	105 subjects (52 males and 53 females; age range 18 to 69 years)	Thresholding for image segmentation. Repeated measurements Regression analysis	Temperature differences between feet (Right Foot-Left Foot) were calculated for each ROI for the thermal imaging device and for the hand-held thermometer. Temperature difference between thermal imaging device and the hand-held thermometer for each predefined ROI : 1 st toe [0.04 (0.30)], 4 th toe [0.03 (0.42)], 1 st metatarsal heads [-0.01 (0.25)], 3 rd metatarsal [0.11 (0.29)] and 5 th metatarsal head [0.21 (0.29)]
4	Maldonado et al., 2020 (153)	<ul style="list-style-type: none"> IR FLUKE TI32 IRT camera 	108 images in total from 17 volunteers	Mask R-CNN model for segmentation	Mean percentage error for area detected by a difference in temperature. This proposed system detects and classifies temperature differences in foot sole zones as ulcerous if >2.2 °C and necrotic if <-2.2 °C. Comparison results among

					different backgrounds (lateral borders, black homogeneous, and non-homogeneous background.)
5	Eid et al., 2018 (154)	<ul style="list-style-type: none"> IR FLIR ONE thermal camera, Additional Equipment: Samsung Note five smartphone, temperature and humidity sensor, tripod, Polyurethane foam, and Accu-Chek Active meter 	five classes/categories of patients: (grade 0: without any signs of complications, grade 1: with local signs of complications (e.g., superficial ulcer), grade 2: with deep complications (e.g., deep ulcer reached to tendon or Charcot's foot), grade 3: with amputation, and grade 4: the healthy volunteers)	Classifiers used for segmentation: (i) k-Nearest Neighbor; (ii) Support vector machine, and Decision tree	Mean absolute temperature difference between the corresponding points of both feet. In case there is no temperature difference (ΔT) $>1.5^{\circ}\text{C}$ between two feet's this refer to normal case, $\Delta T >1.5^{\circ}\text{C}$ refer to grade zero, $\Delta T >2^{\circ}\text{C}$ refer to grade one, $\Delta T >3^{\circ}\text{C}$ refer to grade two and in case there is amputation this refer to grade three diabetic foot.
6	Cruz-Vega et al., 2020 (155)	-	110 thermograms of DM subjects obtained from a public thermogram database were used	Automatic segmentation to obtain the ROI. models based on CNNs were used for multi-class classification of the thermograms. Five categories of the change degree of the plantar regions	Five categories of the change degree of the plantar regions based on Thermal Change Index (TCI) Foot region is divided into four angiosomes: medial plantar artery (MPA), lateral plantar artery (LPA), medial calcaneal artery (MCA), and lateral calcaneal artery (LCA).
7	Vardasca et al., 2019 (156)	<ul style="list-style-type: none"> FLIR® (Wilsoville, OR, USA) E60 thermal camera (FPA sensor array size of 320x240, NETD of $<50\text{mK}$ @ 30°C, measurement uncertainty) 	39 patients, only 14 had infected or ischaemic wound, the other 25 had a healing wound (<i>Centro Hospitalar e Universitario do Porto</i>)	k-NN, SVM, ANN	k-NN of 5 neighbors with 81.25% accuracy, 80% specificity and 100% sensitivity
8	Adam et al., 2018 (157)	Thermographic System VarioCAM© hr head 680/30mm positioned at 1m distance from the feet	51 healthy individuals and 66 diabetic patients (33 with and 33 without neuropathy)	segmented plantar foot thermograms are decomposed into coefficients using double density-dual tree-complex wavelet transform (DD-DT-CWT). Then, k-NN classifier is applied using four LSDA features from bilateral foot thermograms	93.16% accuracy, 90.91% sensitivity and 98.04% specificity

9	Petrova et al., 2020 (152)	The thermal imaging device is a portable two-camera battery-operated instrument for imaging plantar, dorsal, medial and lateral sites of each foot (standard digital RGB +Infrared thermal camera)	People with diabetes (n = 110). Divided into Control group n=61 and Intervention group n = 49, study period 12 months (monthly follow-up study visits for 1 year)	Univariate and multivariate modelling of the likelihood of ulcer recurrence at 12 months	<p>Criteria: A hot spot was defined as an area with a temperature difference between corresponding sites of feet $\geq 2.2^{\circ}\text{C}$.</p> <p>Results: The odds ratios of ulcer recurrence (intervention vs control) were 0.82 (95% CI 0.38, 1.8; P = 0.62) and 0.55 (95% CI 0.21, 1.4; P = 0.22) in univariate and multivariate logistic regression analyses, respectively</p>
10	van Doremalen et al., 2019 (158)	3D foot model and three thermal infrared images using a high-resolution medical 3D imaging system aligned with three smartphone-based thermal infrared cameras. medical 3D imaging system (Vectra XT, Canfield Imaging Systems, Fairfield, NJ, USA) creates 3D models using a passive photogrammetry technique	8 participants with a current diabetic foot ulcer	Creation of 3D thermographs	creation of clinically useful 3D thermal foot images to assess the diabetic foot skin temperature in 3D in a hospital IT environment
11	Astasio-Picado et al., 2019 (159)	The photographic images were made with an infrared camera model FLIR E60bx®	277 patients with diabetic pathology (138 men and 139 women), with an average age of 63.41 ± 17.69 years and a body mass index of 29.08 ± 5.86 , delimited in four groups: 22 (7.94%) with neuropathy, 32 (11.55%) with vasculopathy, 83 (29.96%) with neurovasculopathy and 140 (50.54%) without previous pathology	data obtained were analyzed using the IBM SPSS Statistics 22 statistical program	There were lower temperatures under the 1st metatarsal head, the 5th metatarsal head, the heel, and pulp of the big toe of both left and right feet of the patients in the neuropathy, vasculopathy, and neurovasculopathy groups relative to the group with neither pathology.
12	Yavuz et al., 2019 (160)	FLIR T650sc (FLIR Systems Inc, Wilsonville, Oregon) or Fluke TiR2 (Fluke Corp, Everett, Washington) infrared thermal cameras	Thirty-seven individuals with diabetes were enrolled in this observational case-control study: nine with diabetic neuropathy and ulcer history (DFU), 14 with diabetic neuropathy (DN), and 14 nonneuropathic control participants (DC).	Mean temperatures were determined in four anatomical regions-hallux and medial, central, and lateral forefoot-and separate linear models with specified contrasts among the DFU, DN, and DC groups	The mean temperature reading in each foot region was higher than 30.0°C in the DFU and DN groups and lower than 30.0°C in the DC group. Mean differences were greatest between the DFU and DC groups, ranging from 3.2°C in the medial forefoot to 4.9°C in the hallux.

			Additional info: age, sex, body mass index, ABI, and duration of diabetes indicate group differences in all of the temperature readings	were set to reveal mean differences for each foot region while controlling for group characteristics. four regions on the thermographs: hallux, medial forefoot (first metatarsal head), central forefoot (second and third metatarsal heads), and lateral forefoot (fourth and fifth metatarsal heads)	
1 3	Fraivan et al., 2018 (161)	mobile thermal camera (FLIR ONE) Conditions: Cooled homogeneous background, controlled room temperature (20–25 °C), reflective surfaces Eliminated.	-	Image processing techniques were deployed based on Open CV Library. The procedure of detecting possible ulcers was implemented based on analyzing the thermal distribution on the two feet. Foot sole segmentation method Thresholding (Otsu) (temperature matrix)	The developed application compares the difference between the temperature distribution on the two feet and checks if there is a Mean Temperature Difference (MTD) greater than 2.2oC (the value which indicates a possible ulcer development).
1 4	Neves et al., 2015 (162)	Foot plantar thermal images were acquired through a high-resolution infrared camera (FLIR Systems Inc. Model SC2000; 320 × 240 pixels)	44 volunteers of both genders (22 women and 22 men; 66.70 ± 6.26 years of age) with type 2 diabetes (diagnosed at 11.84 ± 8.22 years), selected among the candidates to Diabetes em Movimento® (a community-based exercise program for patients with type 2 diabetes developed in the city of Vila Real, Portugal)	Three regions of interest (ROI) were defined for evaluation: first finger, fifth finger and the heel. From the three pairs of ROIs evaluated, the higher temperature asymmetry was selected for diabetic foot risk analysis. Pearson's correlations were used to evaluate the association between anthropometric profile variables	Three subjects with diabetes-related foot complications (ROIs higher temperature asymmetry ≥ 2.20 °C) were identified in the sample. All participants with detected diabetes-related foot complications were obese (BMI ≥ 30 kg/m ²) with high levels of body fat (≥ 45%). It can be concluded that exist a positive association either of BMI (r=0.399, p=0.007) either of body fat percentage (r=0.432, p=0.003), with diabetic foot risk in patients with type 2 diabetes.

				(body mass, body height, BMI and body fat) and the higher temperature asymmetry (among the three pairs of ROIs evaluated)	
1 5	Keenan et al., 2017 (163)	infrared camera used was the FLIR A325, which uses an uncooled microbolometer detector. This has a spatial resolution (instantaneous field of view) of 1.36 mrad and sensitivity of 70 mK at 30 °C.	Eleven patients with non-infected foot ulcers were recruited. Three non-diabetic wounds were also investigated in a clinical setting.	This research investigated the emissivity variation of chronic wounds and its effect on thermal measurements. A reflectance based method was used which involved alternating shades at different temperatures over the region of interest. Based on the change in the thermal images, emissivity was calculated at each pixel.	Overall, it was found that the emissivity of wounds was similar or slightly higher to intact skin (range 0.01-0.03 higher with an average value of 0.97 ± 0.03), with lower values at wound edges (on average 0.02 lower than intact skin). Correcting for emissivity resulted in an average temperature difference of 0.83% in the thermal images.

5.1.3 Comparisons

Summary: IRT on DF diagnosis is implemented by establishing a relationship between temperature changes in IRT imaging over different stages of DF evolution for different ROIs (Regions of Interest) in the diabetic foot.

Foot segmentation Algorithms: Different approaches for segmentation and risk zone detection have been utilized in various researches. Some systems use automatic segmentation algorithms and usually require a homogeneous background that simplifies the process, while others prefer a manual segmentation or even use over-segmentation with manual labeling. Different methods of automated segmentation have been analyzed: thresholding, image processing and edge detection algorithms, or even shallow and deep learning clustering and classification techniques.

Infrared Thermal Cameras characteristics: number of pixels (320H x 240V), measuring range (starts from -20 °C and goes up to +150 °C), spectral range (8.0 μm to 14 μm), noise equivalent temperature difference (≤ 0.05 °C at 30 °C target temp (50 mK)), temperature indicating accuracy (± 2 °C or 2 %, whichever is greater [at 25 °C nominal]), field of view (1.2μRad), resolution (>16bit).

Participants: the number of participants varies per study (with an average range value of 50-100 participants, while there is a minimum number of 8-10 participants and a maximum number of 277 participants). The volunteers are divided into various groups with most common division in healthy and diabetic patients. Additional information that is included for analysis, based on researches, could be: age, gender, body mass index (BMI), and blood sugar level (BSL), for each patient.

Criteria: Most of the examined researches and clinical trials classify the temperature differences in foot sole zones as ulcerous if >2.2 °C and non-infected and non-ischemic foot ulcer <2.2 °C.

5.2 Hyperspectral and NIR Spectrum Technologies

5.2.1 Medical Hyperspectral Imaging Fundamentals

Hyperspectral imaging (HSI), also called imaging spectrometer, has its origins in the field of remote sensing. With the advantage of acquiring two-dimensional images across a wide range of electromagnetic spectrum, HSI has been applied to numerous areas including medicine and biomedicine. HSI acquires a three-dimensional dataset called hypercube, with two spatial dimensions and one spectral dimension. Spatially resolved spectral imaging obtained by HSI provides diagnostic information about the tissue physiology, morphology, and composition. As an emerging imaging modality for medical applications, HSI offers great potential for non-invasive disease diagnosis and surgical guidance. It is assumed that the absorption, fluorescence, and scattering characteristics of tissue change during the progression of disease. Therefore, the reflected, fluorescent, and transmitted light from tissue captured by HSI carries quantitative diagnostic information about tissue pathology. Reflectance imaging can detect local changes in scattering and absorption properties of tissue, and fluorescence imaging can probe changes in the biochemical composition of tissue by revealing levels of endogenous fluorophores. Multimodal HSI combining reflectance and fluorescence has been investigated for diagnostic purposes.

HSI is a hybrid modality that combines imaging and spectroscopy. By collecting spectral information at each pixel of a two-dimensional (2D) detector array, HSI generates a three-dimensional (3D) dataset of spatial and spectral information, known as hypercube. With spatial information, the source of each spectrum on samples can be located, which makes it possible to probe more completely the light interactions with pathology. The spectral signature of each pixel in the images enables HSI to identify various pathological conditions. HSI generally covers a contiguous portion of the light spectrum with more spectral bands (up to a few hundreds) and higher spectral resolution than multispectral imaging (such as RGB color cameras). Therefore, HSI has the potential to capture the subtle spectral differences under different pathological conditions, while multispectral imaging may miss significant spectral information for diagnostics.

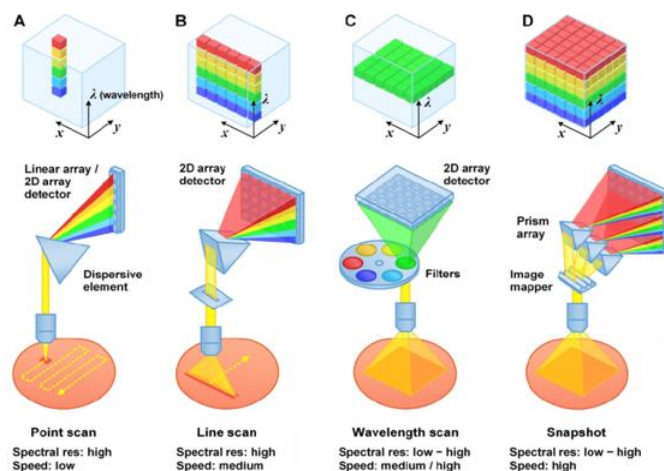


Figure 5-2 Classification of hyperspectral HSI systems based on acquisition mode [Error! Reference source not found.]

5.2.1.1 Acquisition Mode

The fundamental classification scheme of HSI systems is based on the acquisition mode, i.e., how spectral and spatial information is acquired. The conventional HSI system involves two scanning methods: spatial scanning and spectral scanning. Spatial scanning methods generate hyperspectral images by acquiring a complete spectrum for each pixel in the case of whiskbroom (point-scanning) instruments or line of pixels in pushbroom (line-scanning) instruments, and then spatially scanning through the scene. Spectral scanning methods, also called staring or area-scanning imaging, involve capturing the whole scene with 2D detector arrays in a single exposure and then stepping through wavelengths to complete the data cube. Spectral scanning approaches usually store images in band-sequential format, which compromises performance between spatial and spectral information, while spatial scanning stores images either in the form of band interleaved by pixel or band interleaved by line, both of which perform well in spatial and spectral analysis. Whiskbroom and pushbroom HSI do not provide live display of spectral images, which is calculated from the spectra after the completion of the spatial scanning of the corresponding area. Staring HSI scanning through wavelength to build the hypercube has the advantage of displaying live spectral images, which is essential for aiming and focusing. Staring imaging is suitable for stationary applications, such as samples under hyperspectral microscope. Pushbroom and staring imaging modes are two of the most frequently used methods in the literature.

5.2.1.2 Spectral Range

Spectral range refers to the wavelength regions covered by HSI systems. MHSI systems can cover UV, VIS, NIR, and mid-IR spectral ranges based on different medical applications (Table 5-2). The most widely used spectral range in the literature falls in VIS and NIR regions. NIR spectral imaging relies on overtone and combination vibrational bands and low-energy electronic transitions in this region, while MIR imaging records the absorbance of light at the vibrational and rotational frequencies of the atoms within the molecule.

Table 5-2. Spectral Range Examples in HSI Systems

Short name	Full name	Spectral range (nm)
UV	Ultraviolet	200 to 400
VIS	Visible	400 to 780
NIR/near-IR	Near-infrared	780 to 2500
MIR/mid-IR	Mid-infrared	2500 to 25,000

5.2.1.3 Measurement mode

Based on the optical properties of biological tissue, HSI systems can work on reflectance, fluorescence, and transmission modes across the UV, VIS, and NIR regions of the electromagnetic spectrum. The majority of the HSI systems in the literature were implemented on the reflectance mode, which measures the reflectance spectral of samples. In reflection measurement, the detector and the light source are on the same side of the sample, which is assumed to be thick and incapable of transmission. In many cases, fluorescence and reflectance modes are employed together to identify biomolecular and morphologic indicators of various tumors. In transmission mode, light is transmitted through tissue samples from a light source placed below the sample holder and recorded by an imaging spectrograph placed above the sample. Transmission mode is usually used when hyperspectral systems are integrated with microscopes to measure light intensity transmitted through samples.

5.2.1.4 Detector

A detector array or detector FPA is an assemblage of individual detectors located at the focal plane of an imaging system. In HSI, FPA includes 2-D arrays that are designed to measure the intensity of light

transmitted by dispersive devices by converting radiation energy into electrical signals. Detectors can work in a wide spectral range of electromagnetic spectrum based on their spectral responses and application requirements. Selection of a suitable FPA is one of the most important steps in the development of spectrometer. Many parameters that characterize the performance of detector arrays, such as signal-to-noise ratio, dynamic range, spectral quantum efficiency, linearity, and so on, need to be considered when choosing a suitable FPA because the performance of the detector arrays directly determines the image quality. The most widely used detector arrays in the literature are charge-coupled devices (CCDs) because of their high quantum yield and very low dark current.

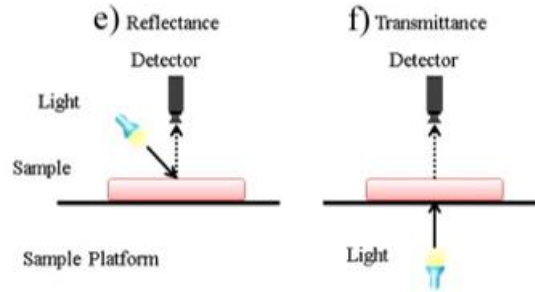


Figure 5-3 Detector examples in HSI

5.2.1.5 Dispersive device

Dispersive devices are the core element of an HSI system, which are either located between the light source and the sample for excitation wavelength selection or between the sample and the detector arrays for emission wavelength dispersion. There are many types of optical and electro-optical dispersive devices, which can perform spectral dispersion or selection in HSI systems. The commonly used dispersive devices in the literature can be divided into three classes: (1) monochromators: prism and diffraction grating, (2) optical bandpass filters: either fixed filter or tunable filters, and (3) single-shot imagers. Optical bandpass filters are either fixed or tunable and are widely used in area-scanning HSI systems. Tunable filters are commonly used in the area-scanning HSI systems, which can be electronically controlled without moving parts and at high tuning speeds. Liquid crystal tunable filter (LCTF) and acousto-optical tunable filter (AOTF) are predominantly utilized in most MHSI systems because of their high image quality and rapid tuning speed over a broad spectral range. LCTFs are generally built by a stack of polarizers and tunable retardation liquid crystal plates. LCTFs work from the VIS to NIR region.

5.2.2 Medical Hyperspectral Images in Diabetic Foot

The studies in Table 5-3 test the ability of medical hyperspectral technology (HT), to quantify tissue oxy- and deoxyhemoglobin to extract information about diabetic foot ulcer. Due to the different absorption spectra of the dominant absorbers, oxy- and deoxyhemoglobin, it is possible to extract information about the oxygen saturation of tissues based on optical measurements such as HSI. The comparison is conducted in four basic categories for each research:

- the equipment used, as well as the environment conditions of the experiment,
- the selected participants (constraints, exclusion/inclusion criteria) and their characteristics (age, gender, etc.),
- the processing strategy that each research follows,
- the results.

Then, a brief outcome, follows, with some conclusions and proposed solutions regarding the good practices and optimal characteristics that we should take into consideration in our case.

Table 5-3 Summary of Literature: Review Table of the Published Works Related to DF Diagnosis with Hyperspectral

Images

A/A	Reference	Basic Equipment and Environmental Conditions	Participants (Number and characteristics)	Image analysis Processing Strategy	Experimental Results
1	Yudovsky et al., 2011 (147)	The illumination optics consisted of seven broadband visible light-emitting diodes [(LEDs), XRE WHT-L1 by CREE Incorporated, Durham, North Caroline] emitting primarily between 500 and 700 nm. The collection optics were composed of (i) a spectral separator (LCTF-10-20 by CRI Incorporated, Woburn, Massachusetts), (ii) a charged-coupled device [(CCD), Guppy F-1468 by Applied Vision Technology, Stadroda, Germany], and (iii) a 25-mm focal-length imaging lens. The spectral separator was tunable over the range of 400–720 nm with a full-width-at-half-maximum (FWHM) value of 10 nm.	66 subjects at the Olive View Medical Center (Olive View-UCLA IRB No. 05H-609300)	Image processing algorithm that automatically classifies ulcers as healing or non-healing. Two classes are created: ulcers that healed within 24 weeks and (ii) ulcers that did not heal within 24 weeks.	The maximum differences (MD) in oxyhemoglobin [MD(OXY)] and deoxyhemoglobin [MD(DEOXY)] concentrations between the target T and the adjacent regions were defined. Retrospective tissue oximetry data from 21 sites affected by ulceration were examined in this study to develop the ulcer prediction index. The algorithm is able to predict tissue at risk of ulceration with a sensitivity and specificity of 95 and 80%, respectively, for images taken, on average, 58 days before tissue damage is apparent to the naked eye. Values $ MD(OXY) > 18$ and $ MD(DEOXY) > 5.8$ with a p-value of < 0.0001 , are significant differences.
2	Khaodhiar et al., 2007 (164)	HyperMed CombiVu-R System (HyperMed, Waltham, MA). HT uses a spectral separator to vary the wavelength of light admitted to a digital detector to provide a spectrum for each pixel—a hyperspectral scan. Tissue spectra are compared with standard spectra for oxy- and deoxyhemoglobin and tissue oxyhemoglobin (HT-oxy) and tissue	Ten type 1 diabetic patients with 21 foot ulcer sites, 13 type 1 diabetic patients without ulcers, and 14 nondiabetic control subjects were seen up to 4 times over a 6-month period.	HT measurements of oxyhemoglobin (HT-oxy) and deoxyhemoglobin (HT-deoxy) were performed at or near the ulcer area and on the upper and lower extremity distant from the ulcer. An HT healing index for each site was calculated from the HT-oxy and -deoxy values.	Hyperspectral tissue oxygenation measurements observed changes in tissue immediately surrounding the ulcer when comparing ulcers that heal and ulcers that do not heal ($P < 0.001$). The sensitivity, specificity, and positive and negative predictive values of the HT index for predicting healing were 93, 86, 93, and 86%, respectively, when evaluated on images taken at the first visit. Changes in HT-oxy among the three

		<p>deoxyhemoglobin (HT-deoxy) determined for each pixel. HT-oxy and -deoxy units represent values for oxyhemoglobin and deoxyhemoglobin found in the tissue volume measured by HTcOM (hyperspectral technology cutaneous oxygenation monitoring). For this study, a 30-s tissue scan was obtained at a 12-inch focal distance and ratioed to a calibration scan obtained using a calibrator (Check Pad; HyperMed) The spatial resolution of the HT images was 60 μm.</p>			<p>risk groups were noted for the metatarsal area of the foot ($P < 0.05$) and the palm ($P < 0.01$). Changes in HT-deoxy and the HT healing index were noted for the palm only ($P < 0.05$ and $P < 0.01$, respectively).</p>
3	<p>Yang et al., 2018 (165)</p>	<p>The HSI setup consists of the following components: Illumination of the foot was via 16×1 W white light-emitting diodes (LEDs) (LXHL-MWEC, LumiledsTM Lighting, San Jose, CA, USA) with 8 units placed on either side of the camera. The HSI camera is a “push-broom” type. The camera comprises a Peltier cooled charge-coupled device (CCD) coupled to an imaging spectrograph (ImSpector V10E, Specim Ltd.). 3D data cube contained 2D spatial images (120×170 pixels) over a wavelength range from 430 nm to 750 nm (272 values).</p>	<p>43 volunteers participated in the clinical study. There were 12 women and 31 men; mean age was 62.7 years. Six of the 43 patients had type 1 diabetes and 37 had type 2 diabetes; 9 were smokers and 39 patients were judged to have neuropathy. Median (range) ankle brachial pressure index (ABPI) was 1.06 (0.15–1.63). Median (range) estimated duration of ulcers prior to assessment was 4.97 (1–26) weeks. 24 healed by 12 weeks and a further 7 healed between 12 and 24 weeks. Ten ulcers did not heal within 24 weeks of follow-up.</p>	<p>SpO2 Data Processing and Principal component analysis was applied. PCA has been applied to a hypercube, with eigenvector and eigenvalue: unfold (a) 3-D datacube into (b) 2-D matrix; (c) obtain eigenvectors and eigenvalues from covariance matrix; (d) multiply the 2-D matrix by the eigenvectors to obtain a score matrix; (e) refold the score matrix to form images at each principal component.</p>	<p>Hyperspectral images from a previous study of 43 patients with wounds were analyzed by using both SpO2 values and PCA, and the principal finding was that classification of time to healing by 12 weeks based on PCA (sensitivity = 87.5%, specificity = 88.2%) outperformed that using SpO2 (sensitivity = 50%, specificity = 88.2%). Comparison by receiver operating characteristic (ROC) analysis revealed an area under the curve of 0.88 for PCA, compared with 0.66 using oxygen saturation analysis. Thus, PCA based on the second principal component appeared superior to analysis using SpO2 values in predicting healing of wounds by 12 weeks based on hyperspectral images taken at baseline.</p>

4	Greenman et al., 2005 (166)	<p>MHSI data were obtained with a HyperMed Visible MHSI System (HyperMed Inc, Watertown, MA, USA). MHSI uses a spectral separator to vary the wavelength of light admitted to a digital camera to provide a spectrum for every pixel—a spectral image. Tissue spectra were compared with standard spectra for oxyhaemoglobin and deoxyhaemoglobin, and total tissue haemoglobin determined for every pixel. A 30-s tissue image was obtained at a 12-inch focal distance and converted to a calibration image by use of a HyperCal-1 calibrator (HyperMed Inc). The spatial resolution of the MHSI images was 60 μm.</p>	<p>108 patients (21 control individuals who did not have diabetes, 36 patients with diabetes who did not have neuropathy, and 51 patients with both diabetes and neuropathy). Medical history assessment included age, sex, weight, height, body-mass index, history of alcohol consumption, type and duration of diabetes, and presence of other microvascular and macrovascular complications.</p>	<p>We used medical hyperspectral imaging (MHSI) to investigate the haemoglobin saturation (S(HSI)O₂; % of oxyhaemoglobin in total haemoglobin [the sum of oxyhaemoglobin and deoxyhaemoglobin]) in the forearm and foot; we also used 31P-MRI scans to study the cellular metabolism of the foot muscles by measuring the concentrations of inorganic phosphate and phosphocreatine and calculating the ratio of inorganic phosphate to phosphocreatine (Pi/PCr).</p>	<p>The forearm S(HSI)O₂ during resting was different in all three groups, with the highest value in controls (mean 42 [SD 17]), followed by the non-neuropathic (32 [SD 8]) and neuropathic (28 [SD 8]) groups ($p < 0.0001$). In the foot at resting, S(HSI)O₂ was higher in the control (38 [22]) and non-neuropathic groups (37 [12]) than in the neuropathic group (30 [12]; $p = 0.027$). The Pi/PCr ratio was higher in the non-neuropathic (0.41 [0.10]) and neuropathic groups (0.58 [0.26]) than in controls (0.20 [0.06]; $p < 0.0001$).</p>
5	Jeffcoate et al., 2015 (167)	-	<p>176 patients with active ulcers were newly referred to the service during the recruitment period, but 126 were either excluded on the grounds of general ill health or frailty, problems with mobility or because they declined to participate. Of the remaining 50 patients, three were studied before a protocol modification, and two were recruited in error</p>	<p>HSI technique was used for healing prediction in routine practice. A novel software accounts for tissue scattering of light, and was validated using blood samples of varying oxygen saturation assessed by blood gas analysis. HSI was then performed on a population newly presenting with diabetic foot ulcers to a specialist clinic, and associations were sought with healing at 12 and 24 weeks.</p>	<p>The correlation between the results of HSI and blood gas analysis was strong ($r = 0.994$). A total of 43 patients (mean \pm sd age 62.7 ± 12.2 years; 31 men, 12 women; 37 with Type 2 diabetes, six with Type 1 diabetes) with foot ulcers were included in the prospective clinical study and underwent HSI within 16 days of presentation. In all, 26 ulcers healed within 12 weeks and 28 within 24 weeks. There was a negative association between tissue oxygenation assessed by HSI at baseline and healing by 12 weeks ($P = 0.009$), and this was observed in both infected</p>

					and non-infected ulcers. There was a significant positive correlation between oxygenation assessed by HSI and time to healing (P = 0.03). No correlations were observed at 24 weeks.
6	Nouvong et al., 2009 (168)	The HSI system obtains multiple images at discrete wavelengths, providing a diffuse reflectance spectrum for each pixel in the image. The system uses wavelengths between 500 and 660 nm to include oxy and deoxy absorption peaks.	<p>Fifty-four patients with 73 ulcers completed the study; at 24 weeks, 54 ulcers healed while 19 ulcers did not heal. Patients aged 21–85 years diagnosed with type 1 or type 2 diabetes with at least one DFU were eligible.</p> <p>Exclusion Criteria: Exclusion criteria included heart failure with consequent lower-extremity edema, stroke or ischemic attack with residual nerve dysfunction, uncontrolled hypertension, end-stage renal disease/renal transplant, peripheral arterial disease that was severe enough to require surgery, severe peripheral edema, any other serious chronic disease that can affect wound healing, treatment with antineoplastic drugs or glucocorticoids, and pregnant or lactating women.</p>	The data were analyzed to detect differences between patients with DFUs that healed and those with DFUs that did not heal. For categorical factors such as sex, differences between the healed and non healed proportions were compared with the χ^2 test. For continuous factors such as oxy, deoxy, and StO ₂ , differences between the means of the two groups were compared with the Student's t test using the more conservative test assuming unequal variances. Values were reported as means \pm SD. A P value <0.05 was considered significant. Sensitivity, specificity, and positive predictive values for healing were calculated using standard definitions. Linear discriminant analysis was used to develop the threshold for separating the healed and non healed groups.	Fifty-four patients with 73 ulcers completed the study; at 24 weeks, 54 ulcers healed while 19 ulcers did not heal. When using the healing index to predict healing, the sensitivity was 80% (43 of 54), the specificity was 74% (14 of 19), and the positive predictive value was 90% (43 of 48). The sensitivity, specificity, and positive predictive values increased to 86, 88, and 96%, respectively, when removing three false-positive osteomyelitis cases and four false-negative cases due to measurements on a callus. The results indicate that cutaneous tissue oxygenation correlates with wound healing in diabetic patients.

5.2.3 Comparisons

Summary: HSI is used to extract information about the oxygen saturation of foot tissues based on optical measurements. **Signal Processing Algorithms:** HSI preprocessing mainly involves data normalization and image registration. Gaussian filter was also used in the literature to smooth spectral signatures and reduce the noise effect. For hyperspectral datasets, a larger number of spectral bands may potentially make the

discrimination between more detailed classes possible. But due to the curse of dimensionality, too many spectral bands used in classification may decrease the classification accuracy. The most widely used dimensionality reduction method for medical hyperspectral dataset analysis is principle component analysis (PCA). Then, techniques such as vector machines (SVMs) and artificial neural networks (ANN) or even Convolutional Neural Networks are widely used for medical hyperspectral image classification.

HSI System Characteristics: Table 5-4 shows examples about the representative hyperspectral imaging systems characteristics for diabetic foot.

Participants: the number of participants varies per study (with an average range value of 50-100 participants, while there is a minimum number of 43 participants and a maximum number of 176 participants). Exclusion criteria included heart failure with consequent lower-extremity edema, stroke or ischemic attack with residual nerve dysfunction, uncontrolled hypertension, end-stage renal disease/renal transplant, peripheral arterial disease that was severe enough to require surgery, severe peripheral edema, any other serious chronic disease that can affect wound healing, treatment with antineoplastic drugs or glucocorticoids, and pregnant or lactating women.

Table 5-4. HSI Systems Characteristics in Diabetic Foot Ulceration

Reference	Spectral Range (nm)	Detector	Dispersive device	Acquisition mode	Measurement mode
Greenman et al, 2005(166)	500 to 600	CCD	LCTF	Staring	Reflectance
Yudovsky et al, 2011(147)	400 to 720	CCD	LCTF	Staring	Reflectance

5.3 Mid-IR Spectrum Technologies

Table 5-5. Summary of Literature: Review Table of the Published Works Related to DF Diagnosis with RGB Or Mid-IR Images.

A/A	Reference	Basic Equipment and Environmental Conditions	Participants (Number and characteristics)	Image analysis Processing Strategy	Experimental Results
1	Kottman et al., 2012 (169)	Quantum Cascade Laser (EC-QCL) (Daylight Solutions DLS-TLS-001-PL), tunable in 0.9 cm^{-1} wavenumber steps from $1010 - 1095 \text{ cm}^{-1}$ via the external grating. QCL chip covers a range of glucose absorption in the Mid-IR . The maximal average laser power lies between 20 mW and 130 mW. A mechanical chopper (New Focus Model 3501) modulates the continuous-wave (cw) laser light, which is focused by several	Epidermal sheets were isolated from forskins obtained from the University Childrens Hospital of Zurich after routine circumcisions. All patients (and/or their parents) gave their written consent for this study in accordance with the Ethics Commission of the Canton Zurich (notification no. StV-12/06)	Glucose detection in epidermal skin samples. The purpose of this paper is to examine blood glucose extraction methods in addition to indicators of blood glucose level, toward development of an innovative, non-invasive extraction technology. Decision support methods are also analyzed toward customized, automated, and intelligent diabetic management.	The PhotoAcoustic (PA) signal linearly depends on the glucose concentration within the large concentration range of 0 to 10 g/dl. the dual-wavelength approach yields a considerably improved stability and an uncertainty of only $\pm 30 \text{ mg/dL}$ of the blood glucose concentration level at a confidence level of 90%.

		anti-reflection coated ZnSe lenses into the PA cell.			
2	Goyal et al., 2018 (170)	RGB three cameras mainly used for capturing the foot images, Kodak DX4530, Nikon D3300 and Nikon COOLPIX P100.	Foot images with DFU were collected from the Lancashire Teaching Hospitals over the past few years. Our dataset has a total of 1775 foot images with DFU.	Faster-RCNN and R-FCN deep learning methods used for image localization. Detection of DFU on foot images (variations in terms of color, size, shape, texture and site amongst different classes of DFU.)	Mean average precision(mAP) considering a correct detection of foot ulcer. mAP = 90.1%

6 Suggested photonic oriented clinical indexes for diabetic ulcer management

Diabetic foot represents a significant cause of severe morbidity in diabetic patients with markedly increased cost to the health care system. Prevention and early diagnosis are the keys to decrease the prevalence of diabetic foot. Self foot-assessment is the main tool for early diagnosis. Use of an objective tool to assess the foot of a diabetic patient in order to predict and early diagnose diabetic foot is essential.

Currently, self foot-assessment is based on patient's optical assessment of his/her own foot and this is subject to extreme variability due to various reasons: patient's difficulty to perform a proper examination, or lack of objectivity / patient's subjective assessment of the foot condition.

The PHOOTONICS project aims to provide two different devices, the Home and the Pro version that will help both patients and health-care professional on early diagnosis and care of this group of people. With the PHOOTONICS-Home patients will be able to have a quick, easy to use and objective self-assessment device which will give them an early notice when a DFU is about to develop.

Based on this review, we assume that the main indices that could be assessed or measured using high-end technology are the following:

- Foot temperature (Home)
- Arterial perfusion (Pro)
- Skin oxygen saturation / deoxyhemoglobin measurement (Pro)
- Plantar pressure distribution (Pro)
- Skin / subcutaneous tissue biochemical composition (water, glucose concentration) (Pro)
- Foot imaging, to detect sites of infection, cracks, fissures, deformities, ulcers, necrosis, footprints (Pro)

Ten sites of the plantar and dorsal foot surface are proposed for measurements with PHOOTONICS device. These are the sites which will also be clinically assessed in terms of temperature, skin lesions, sensation and perfusion.

In detail, the plantar surface of 1st, 3rd, 5th digit (1,2,3 of the image), the plantar surface of the 1st, 3rd, 5th metatarsal (4,5,6), the middle internal and lateral plantar surface (7,8), the plantar heel surface (9), the dorsal surface of the 1st metatarsal (10) are the proposed sites for PHOOTONICS devices measurement.



If possible, dermatoglyphics of both feet/all toes and both hands/all fingers may be integrated for the prediction and assessment of disease. This has not been shown yet for diabetes, but for other diseases e.g. cancer (171).

Table 6-1. Outcomes for Photonics Based Diagnostic Tests

Imaging	Measurements	Algorithms	Sensors/Camers	Participants	Criteria
Infrared/ Thermal	Temperature	Classification, clustering, image processing and edge detection algorithms	Pixels (320H x 240V), measuring range (starts from -20 °C and goes up to +150 °C), spectral range (8.0 μm to 14 μm), noise equivalent temperature difference (≤ 0.05 °C at 30 °C target temp (50 mK)), temperature indicating accuracy (± 2 °C or 2 %, whichever is greater [at 25 °C nominal]), field of view (1.2μRad), resolution (>16bit).	Varying number, in most cases 50-100 participants Additional information that is included for analysis, based on researches, could be: age, gender, body mass index (BMI), and blood sugar level (BSL), for each patient	Classify the temperature differences in foot sole zones as ulcerous if >2.2 °C and noninfected and nonischemic foot ulcer <2.2 °C.
Hyperspectral	Oxygen saturation of foot tissues based on optical measurements	Principle component analysis (PCA) and techniques such as vector machines (SVMs) and artificial neural networks (ANN) or even Convolutional Neural Networks	Spectral range: 400 to 720 nm Detector: CCD Dispersive device: LCTF Acquisition Mode: Staring Measurement Mode: Reflectance	Exclusion criteria included heart failure with consequent lower-extremity edema, stroke or ischemic attack with residual nerve dysfunction, uncontrolled hypertension, end-stage renal disease/renal transplant, severe peripheral arterial disease, severe peripheral edema, any	Differences (D) in oxyhemoglobin [D(OXY)] >18 and deoxyhemoglobin [D(DEOXY)] >5.8 concentrations between the target T and the adjacent regions are significant

				other serious chronic disease, treatment with antineoplastic drugs or glucocorticoids, and pregnant or lactating women.	
Mid-IR	Glucose concentration	Signal processing and statistical methods	Quantum Cascade Laser (EC-QCL) (Daylight Solutions DLS-TLS-001-PL), tunable in 0.9 cm ⁻¹ wavenumber steps from 1010 – 1095 cm ⁻¹ via the external grating. QCL chip covers a range of glucose absorption in the Mid-IR.	-	the glucose concentration with range of 0 to 10 g/dl is considered as large concentration.

References

1. Bus SA, van Netten JJ. A shift in priority in diabetic foot care and research: 75% of foot ulcers are preventable. *Diabetes Metab Res Rev.* 2016 Jan;32 Suppl 1:195-200.
2. Brownrigg JR, Apelqvist J, Bakker K, Schaper NC, Hinchliffe RJ. Evidence-based management of PAD & the diabetic foot. *Eur J Vasc Endovasc Surg.* 2013 Jun;45(6):673-81.
3. Driver VR, Fabbi M, Lavery LA, Gibbons G. The costs of diabetic foot: the economic case for the limb salvage team. *J Vasc Surg.* 2010 Sep;52(3 Suppl):17S-22S.
4. Bus SA. Innovations in plantar pressure and foot temperature measurements in diabetes. *Diabetes Metab Res Rev.* 2016 Jan;32 Suppl 1:221-6.
5. Kumar S, Ashe HA, Parnell LN, Fernando DJ, Tsigos C, Young RJ, et al. The prevalence of foot ulceration and its correlates in type 2 diabetic patients: a population-based study. *Diabet Med.* 1994 Jun;11(5):480-4.
6. Boulton AJ. The pathway to foot ulceration in diabetes. *Med Clin North Am.* 2013 Sep;97(5):775-90.
7. Krentz AJ, Acheson P, Basu A, Kilvert A, Wright AD, M. N. Morbidity and mortality associated with diabetic foot disease: A 12-month prospective survey of hospital admissions in a single UK centre. *Endocrinology, Diabetes, Metabolism, and Nutrition.* 1997;7(3):144-7.
8. Abbott CA, Carrington AL, Ashe H, Bath S, Every LC, Griffiths J, et al. The North-West Diabetes Foot Care Study: incidence of, and risk factors for, new diabetic foot ulceration in a community-based patient cohort. *Diabet Med.* 2002 May;19(5):377-84.
9. Muller IS, de Grauw WJ, van Gerwen WH, Bartelink ML, van Den Hoogen HJ, Rutten GE. Foot ulceration and lower limb amputation in type 2 diabetic patients in dutch primary health care. *Diabetes Care.* 2002 Mar;25(3):570-4.
10. Singh N, Armstrong DG, Lipsky BA. Preventing foot ulcers in patients with diabetes. *JAMA.* 2005 Jan 12;293(2):217-28.
11. Boulton AJ, Vileikyte L, Ragnarson-Tennvall G, Apelqvist J. The global burden of diabetic foot disease. *Lancet.* 2005 Nov 12;366(9498):1719-24.
12. Lavery LA, Ashry HR, van Houtum W, Pugh JA, Harkless LB, Basu S. Variation in the incidence and proportion of diabetes-related amputations in minorities. *Diabetes Care.* 1996 Jan;19(1):48-52.
13. Lavery LA, van Houtum WH, Harkless LB. In-hospital mortality and disposition of diabetic amputees in The Netherlands. *Diabet Med.* 1996 Feb;13(2):192-7.
14. Chevreur K, Berg Brigham K, Bouch[√]© C. The burden and treatment of diabetes in France. *Global Health.* 2014 Feb 20;10:6.
15. Veves A, Van Ross ER, Boulton AJ. Foot pressure measurements in diabetic and nondiabetic amputees. *Diabetes Care.* 1992 Jul;15(7):905-7.
16. Armstrong DG, Wrobel J, Robbins JM. Guest Editorial: are diabetes-related wounds and amputations worse than cancer? *Int Wound J.* 2007 Dec;4(4):286-7.
17. Mayfield JA, Reiber GE, Maynard C, Czerniecki JM, Caps MT, Sangeorzan BJ. Survival following lower-limb amputation in a veteran population. *J Rehabil Res Dev.* 2001 May-Jun;38(3):341-5.
18. Van Acker K, Oleen-Burkey M, De Decker L, Vanmaele R, Van Schil P, Matricali G, et al. Cost and resource utilization for prevention and treatment of foot lesions in a diabetic foot clinic in Belgium. *Diabetes Res Clin Pract.* 2000 Oct;50(2):87-95.
19. Rigato M, Pizzol D, Tiago A, Putoto G, Avogaro A, Fadini GP. Characteristics, prevalence, and outcomes of diabetic foot ulcers in Africa. A systemic review and meta-analysis. *Diabetes Res Clin Pract.* 2018 Aug;142:63-73.

20. Younis BB, Shahid A, Arshad R, Khurshid S, Ahmad M, Yousaf H. Frequency of foot ulcers in people with type 2 diabetes, presenting to specialist diabetes clinic at a Tertiary Care Hospital, Lahore, Pakistan. *BMC Endocr Disord.* 2018 Aug 6;18(1):53.
21. Boyko EJ, Ahroni JH, Cohen V, Nelson KM, Heagerty PJ. Prediction of diabetic foot ulcer occurrence using commonly available clinical information: the Seattle Diabetic Foot Study. *Diabetes Care.* 2006 Jun;29(6):1202-7.
22. Frykberg RG, Gordon IL, Reyzelman AM, Cazzell SM, Fitzgerald RH, Rothenberg GM, et al. Feasibility and Efficacy of a Smart Mat Technology to Predict Development of Diabetic Plantar Ulcers. *Diabetes Care.* 2017 Jul;40(7):973-80.
23. Kastenbauer T, Sauseng S, Sokol G, Auinger M, Irsigler K. A prospective study of predictors for foot ulceration in type 2 diabetes. *J Am Podiatr Med Assoc.* 2001 Jul-Aug;91(7):343-50.
24. Monteiro-Soares M, Dinis-Ribeiro M. External validation and optimisation of a model for predicting foot ulcers in patients with diabetes. *Diabetologia.* 2010 Jul;53(7):1525-33.
25. Monteiro-Soares M, Ribas R, Pereira da Silva C, Bral T, Mota A, Pinheiro Torres S, et al. Diabetic foot ulcer development risk classifications' validation: A multicentre prospective cohort study. *Diabetes Res Clin Pract.* 2017 May;127:105-14.
26. Murray HJ, Young MJ, Hollis S, Boulton AJ. The association between callus formation, high pressures and neuropathy in diabetic foot ulceration. *Diabet Med.* 1996 Nov;13(11):979-82.
27. Pham H, Armstrong DG, Harvey C, Harkless LB, Giurini JM, Veves A. Screening techniques to identify people at high risk for diabetic foot ulceration: a prospective multicenter trial. *Diabetes Care.* 2000 May;23(5):606-11.
28. Sosenko JM, Kato M, Soto R, Bild DE. Comparison of quantitative sensory-threshold measures for their association with foot ulceration in diabetic patients. *Diabetes Care.* 1990 Oct;13(10):1057-61.
29. Yun JS, Cha SA, Lim TS, Lee EY, Song KH, Ahn YB, et al. Cardiovascular Autonomic Dysfunction Predicts Diabetic Foot Ulcers in Patients With Type 2 Diabetes Without Diabetic Polyneuropathy. *Medicine (Baltimore).* 2016 Mar;95(12):e3128.
30. Frykberg RG, Zgonis T, Armstrong DG, Driver VR, Giurini JM, Kravitz SR, et al. Diabetic foot disorders. A clinical practice guideline (2006 revision). *J Foot Ankle Surg.* 2006 Sep-Oct;45(5 Suppl):S1-66.
31. Lavery LA, Armstrong DG, Wunderlich RP, Tredwell J, Boulton AJ. Predictive value of foot pressure assessment as part of a population-based diabetes disease management program. *Diabetes Care.* 2003 Apr;26(4):1069-73.
32. Boulton AJ, Armstrong DG, Albert SF, Frykberg RG, Hellman R, Kirkman MS, et al. Comprehensive foot examination and risk assessment: a report of the task force of the foot care interest group of the American Diabetes Association, with endorsement by the American Association of Clinical Endocrinologists. *Diabetes Care.* 2008 Aug;31(8):1679-85.
33. Jeffcoate WJ, Harding KG. Diabetic foot ulcers. *Lancet.* 2003 May 3;361(9368):1545-51.
34. Allison MA, Criqui MH, McClelland RL, Scott JM, McDermott MM, Liu K, et al. The effect of novel cardiovascular risk factors on the ethnic-specific odds for peripheral arterial disease in the Multi-Ethnic Study of Atherosclerosis (MESA). *J Am Coll Cardiol.* 2006 Sep 19;48(6):1190-7.
35. Meijer WT, Hoes AW, Rutgers D, Bots ML, Hofman A, Grobbee DE. Peripheral arterial disease in the elderly: The Rotterdam Study. *Arterioscler Thromb Vasc Biol.* 1998 Feb;18(2):185-92.
36. Newman AB, Siscovick DS, Manolio TA, Polak J, Fried LP, Borhani NO, et al. Ankle-arm index as a marker of atherosclerosis in the Cardiovascular Health Study. *Cardiovascular Heart Study (CHS) Collaborative Research Group. Circulation.* 1993 Sep;88(3):837-45.
37. Morbach S, Furchert H, Gröbblinghoff U, Hoffmeier H, Kersten K, Klauke GT, et al. Long-term prognosis of diabetic foot patients and their limbs: amputation and death over the course of a decade. *Diabetes Care.* 2012 Oct;35(10):2021-7.

38. Prompers L, Huijberts M, Apelqvist J, Jude E, Piaggese A, Bakker K, et al. High prevalence of ischaemia, infection and serious comorbidity in patients with diabetic foot disease in Europe. Baseline results from the Eurodiale study. *Diabetologia*. 2007 Jan;50(1):18-25.
39. Boulton AJ, Gries FA, Jervell JA. Guidelines for the diagnosis and outpatient management of diabetic peripheral neuropathy. *Diabet Med*. 1998 Jun;15(6):508-14.
40. Dyck PJ, Kratz KM, Karnes JL, Litchy WJ, Klein R, Pach JM, et al. The prevalence by staged severity of various types of diabetic neuropathy, retinopathy, and nephropathy in a population-based cohort: the Rochester Diabetic Neuropathy Study. *Neurology*. 1993 Apr;43(4):817-24.
41. Rith-Najarian SJ, Stolusky T, Gohdes DM. Identifying diabetic patients at high risk for lower-extremity amputation in a primary health care setting. A prospective evaluation of simple screening criteria. *Diabetes Care*. 1992 Oct;15(10):1386-9.
42. Smith AG, Singleton JR. Impaired glucose tolerance and neuropathy. *Neurologist*. 2008 Jan;14(1):23-9.
43. Jorreskog G. Why critical limb ischemia criteria are not applicable to diabetic foot and what the consequences are. *Scand J Surg*. 2012;101(2):114-8.
44. Cao P, Eckstein HH, De Rango P, Setacci C, Ricco JB, de Donato G, et al. Chapter II: Diagnostic methods. *Eur J Vasc Endovasc Surg*. 2011 Dec;42 Suppl 2:S13-32.
45. Hinchliffe RJ, Forsythe RO, Apelqvist J, Boyko EJ, Fitridge R, Hong JP, et al. Guidelines on diagnosis, prognosis, and management of peripheral artery disease in patients with foot ulcers and diabetes (IWGDF 2019 update). *Diabetes Metab Res Rev*. 2020 Mar;36 Suppl 1:e3276.
46. Wang Z, Hasan R, Firwana B, Elraiyah T, Tsapas A, Prokop L, et al. A systematic review and meta-analysis of tests to predict wound healing in diabetic foot. *J Vasc Surg*. 2016 Feb;63(2 Suppl):29S-36S e1-2.
47. McDermott MM, Applegate WB, Bonds DE, Buford TW, Church T, Espeland MA, et al. Ankle brachial index values, leg symptoms, and functional performance among community-dwelling older men and women in the lifestyle interventions and independence for elders study. *J Am Heart Assoc*. 2013 Nov 12;2(6):e000257.
48. McDermott MM, Guralnik JM, Ferrucci L, Tian L, Liu K, Liao Y, et al. Asymptomatic peripheral arterial disease is associated with more adverse lower extremity characteristics than intermittent claudication. *Circulation*. 2008 May 13;117(19):2484-91.
49. Boyko EJ, Ahroni JH, Davignon D, Stensel V, Prigeon RL, Smith DG. Diagnostic utility of the history and physical examination for peripheral vascular disease among patients with diabetes mellitus. *J Clin Epidemiol*. 1997 Jun;50(6):659-68.
50. Dolan NC, Liu K, Criqui MH, Greenland P, Guralnik JM, Chan C, et al. Peripheral artery disease, diabetes, and reduced lower extremity functioning. *Diabetes Care*. 2002 Jan;25(1):113-20.
51. Crawford F, Cezard G, Chappell FM. The development and validation of a multivariable prognostic model to predict foot ulceration in diabetes using a systematic review and individual patient data meta-analyses. *Diabet Med*. 2018 Nov;35(11):1480-93.
52. Game FL, Chipchase SY, Hubbard R, Burden RP, Jeffcoate WJ. Temporal association between the incidence of foot ulceration and the start of dialysis in diabetes mellitus. *Nephrol Dial Transplant*. 2006 Nov;21(11):3207-10.
53. Ndip A, Lavery LA, Lafontaine J, Rutter MK, Vardhan A, Vileikyte L, et al. High levels of foot ulceration and amputation risk in a multiracial cohort of diabetic patients on dialysis therapy. *Diabetes Care*. 2010 Apr;33(4):878-80.
54. Ndip A, Rutter MK, Vileikyte L, Vardhan A, Asari A, Jameel M, et al. Dialysis treatment is an independent risk factor for foot ulceration in patients with diabetes and stage 4 or 5 chronic kidney disease. *Diabetes Care*. 2010 Aug;33(8):1811-6.
55. Abbott CA, Garrow AP, Carrington AL, Morris J, Van Ross ER, Boulton AJ. Foot ulcer risk is

- lower in South-Asian and african-Caribbean compared with European diabetic patients in the U.K.: the North-West diabetes foot care study. *Diabetes Care*. 2005 Aug;28(8):1869-75.
56. Reiber GE, Vileikyte L, Boyko EJ, del Aguila M, Smith DG, Lavery LA, et al. Causal pathways for incident lower-extremity ulcers in patients with diabetes from two settings. *Diabetes Care*. 1999 Jan;22(1):157-62.
 57. Andros G, Lavery LA. Diabetic Foot Ulcers. In: Cronenwett JL, Johnston KW, editors. *Rutherford's Vascular Surgery*. 7th ed. Philadelphia: Saunders Elsevier; 2010. p. 1735-46.
 58. Ragnarson Tennvall G, Apelqvist J. Health-economic consequences of diabetic foot lesions. *Clin Infect Dis*. 2004 Aug 1;39 Suppl 2:S132-9.
 59. Barshes NR, Sigireddi M, Wrobel JS, Mahankali A, Robbins JM, Koungias P, et al. The system of care for the diabetic foot: objectives, outcomes, and opportunities. *Diabet Foot Ankle*. 2013 Oct 10;4.
 60. Kerr M, Rayman G, Jeffcoate WJ. Cost of diabetic foot disease to the National Health Service in England. *Diabet Med*. 2014 Dec;31(12):1498-504.
 61. Rice JB, Desai U, Cummings AK, Birnbaum HG, Skornicki M, Parsons NB. Burden of diabetic foot ulcers for medicare and private insurers. *Diabetes Care*. 2014;37(3):651-8.
 62. Keskek SO, Kirim S, Yanmaz N. Estimated costs of the treatment of diabetic foot ulcers in a tertiary hospital in Turkey. *Pak J Med Sci*. 2014 Sep;30(5):968-71.
 63. Ramsey SD, Newton K, Blough D, McCulloch DK, Sandhu N, Reiber GE, et al. Incidence, outcomes, and cost of foot ulcers in patients with diabetes. *Diabetes Care*. 1999 Mar;22(3):382-7.
 64. Hicks CW, Selvarajah S, Mathioudakis N, Sherman RE, Hines KF, Black JH, 3rd, et al. Burden of Infected Diabetic Foot Ulcers on Hospital Admissions and Costs. *Ann Vasc Surg*. 2016 May;33:149-58.
 65. NICE, Guidance. Diabetic foot problems: prevention and management. NICE guideline [NG19]. National Institute for Health and Care Excellence; 2019 [updated 11 October 2019]; Available from: <https://www.nice.org.uk/guidance/ng19>.
 66. Kuhnke J, Botros M, Elliot J, Rodd-Nielse E, Orsted H, Sibbald G. The case for diabetic foot screening. *Diabetic Foot Canada*. 2013;1(2):8-14.
 67. Formosa C, Gatt A, Chockalingam N. A Critical Evaluation of Existing Diabetic Foot Screening Guidelines. *Rev Diabet Stud*. 2016 Summer-Fall;13(2-3):158-86.
 68. Bowering CK. Diabetic foot ulcers. Pathophysiology, assessment, and therapy. *Can Fam Physician*. 2001 May;47:1007-16.
 69. Dyck PJ, Davies JL, Wilson DM, Service FJ, Melton LJ, 3rd, O'Brien PC. Risk factors for severity of diabetic polyneuropathy: intensive longitudinal assessment of the Rochester Diabetic Neuropathy Study cohort. *Diabetes Care*. 1999 Sep;22(9):1479-86.
 70. Feldman EL, Russell JW, Sullivan KA, Golovoy D. New insights into the pathogenesis of diabetic neuropathy. *Curr Opin Neurol*. 1999 Oct;12(5):553-63.
 71. Simmons Z, Feldman EL. Update on diabetic neuropathy. *Curr Opin Neurol*. 2002 Oct;15(5):595-603.
 72. Zochodne DW. Diabetic polyneuropathy: an update. *Curr Opin Neurol*. 2008 Oct;21(5):527-33.
 73. Clayton WJ, Elasy TA. A Review of the Pathophysiology, Classification, and Treatment of Foot Ulcers in Diabetic Patients. *Clinical Diabetes*. 2009;27(2):52-8.
 74. Huijberts MS, Schaper NC, Schalkwijk CG. Advanced glycation end products and diabetic foot disease. *Diabetes Metab Res Rev*. 2008 May-Jun;24 Suppl 1:S19-24.
 75. Paraskevas KI, Baker DM, Pompella A, Mikhailidis DP. Does diabetes mellitus play a role in restenosis and patency rates following lower extremity peripheral arterial revascularization? A critical overview. *Ann Vasc Surg*. 2008 May-Jun;22(3):481-91.
 76. Armstrong DG, Lavery LA. Diabetic foot ulcers: prevention, diagnosis and classification. *Am Fam Physician*. 1998 Mar 15;57(6):1325-32, 37-8.
 77. Lavery LA, Armstrong DG, Wunderlich RP, Mohler MJ, Wendel CS, Lipsky BA. Risk factors for

- foot infections in individuals with diabetes. *Diabetes Care*. 2006 Jun;29(6):1288-93.
78. Leese GP, Cochrane L, Mackie AD, Stang D, Brown K, Green V. Measuring the accuracy of different ways to identify the 'at-risk' foot in routine clinical practice. *Diabet Med*. 2011 Jun;28(6):747-54.
79. Brownrigg JR, Hinchliffe RJ, Apelqvist J, Boyko EJ, Fitridge R, Mills JL, et al. Effectiveness of bedside investigations to diagnose peripheral artery disease among people with diabetes mellitus: a systematic review. *Diabetes Metab Res Rev*. 2016 Jan;32 Suppl 1:119-27.
80. Leoniuk J, Lukasiewicz A, Szorc M, Sackiewicz I, Janica J, Lebkowska U. Doppler ultrasound detection of preclinical changes in foot arteries in early stage of type 2 diabetes. *Pol J Radiol*. 2014;79:283-9.
81. Bus SA, van Netten JJ, Lavery LA, Monteiro-Soares M, Rasmussen A, Jubiz Y, et al. IWGDF guidance on the prevention of foot ulcers in at-risk patients with diabetes. *Diabetes Metab Res Rev*. 2016 Jan;32 Suppl 1:16-24.
82. Bus SA, Lavery LA, Raspovic A, Sacco ICN, van Netten JJ. IWGDF Guideline on the prevention of foot ulcers in persons with diabetes. 2019; Available from: <https://iwgdfguidelines.org/wp-content/uploads/2019/05/02-IWGDF-prevention-guideline-2019.pdf>.
83. Peripheral arterial disease in people with diabetes. *Diabetes Care*. 2003 Dec;26(12):3333-41.
84. Chaudru S, de M^vllenheim PY, Le Faucheur A, Kaladji A, Jaquinandi V, Mah^v© G. Training to Perform Ankle-Brachial Index: Systematic Review and Perspectives to Improve Teaching and Learning. *Eur J Vasc Endovasc Surg*. 2016 Feb;51(2):240-7.
85. Haigh KJ, Bingley J, Golledge J, Walker PJ. Barriers to screening and diagnosis of peripheral artery disease by general practitioners. *Vasc Med*. 2013 Dec;18(6):325-30.
86. Mohler ER, 3rd, Treat-Jacobson D, Reilly MP, Cunningham KE, Miani M, Criqui MH, et al. Utility and barriers to performance of the ankle-brachial index in primary care practice. *Vasc Med*. 2004 Nov;9(4):253-60.
87. Forsythe RO, Hinchliffe RJ. Assessment of foot perfusion in patients with a diabetic foot ulcer. *Diabetes Metab Res Rev*. 2016 Jan;32 Suppl 1:232-8.
88. Normahani P, Mustafa C, Standfield NJ, Duguid C, Fox M, Jaffer U. Management of peripheral arterial disease in diabetes: a national survey of podiatry practice in the United Kingdom. *J Foot Ankle Res*. 2018;11:29.
89. Vriens B, D'Abate F, Ozdemir BA, Fenner C, Maynard W, Budge J, et al. Clinical examination and non-invasive screening tests in the diagnosis of peripheral artery disease in people with diabetes-related foot ulceration. *Diabet Med*. 2018 Jul;35(7):895-902.
90. Dinh T, Tecilazich F, Kafanas A, Doupis J, Gnardellis C, Leal E, et al. Mechanisms involved in the development and healing of diabetic foot ulceration. *Diabetes*. 2012 Nov;61(11):2937-47.
91. Monofilament testing for loss of protective sensation of diabetic/neuropathic feet for adults and children. British Columbia Provincial Nursing Skin and Wound Committee; [updated May 2014]; Available from: <https://www.clwk.ca/buddydrive/file/procedure-monofilament-testing/?download=106%25Aprocedure-monofilament-testing-for-lops>.
92. Viswanathan V, Chamukuttan S, Rajsekar S, Ramachandran A. The Rydel Seiffer tuning fork: An inexpensive device for screening diabetic patients with high-risk foot. *Practical Diabetes International*. 2001;18(5):155-6.
93. Mishra SC, Chhatbar KC, Kashikar A, Mehndiratta A. Diabetic foot. *BMJ*. 2017 Nov 16;359:j5064.
94. Herity NA, Ward MR, Lo S, Yeung AC. Review: Clinical aspects of vascular remodeling. *J Cardiovasc Electrophysiol*. 1999 Jul;10(7):1016-24.
95. Reddy HK, Koshy SK, Foerst J, Sturek M. Remodeling of coronary arteries in diabetic patients-an intravascular ultrasound study. *Echocardiography*. 2004 Feb;21(2):139-44.
96. Endemann DH, Pu Q, De Ciuceis C, Savoia C, Viridis A, Neves MF, et al. Persistent remodeling of resistance arteries in type 2 diabetic patients on antihypertensive treatment. *Hypertension*. 2004

Feb;43(2):399-404.

97. Schofield I, Malik R, Izzard A, Austin C, Heagerty A. Vascular structural and functional changes in type 2 diabetes mellitus: evidence for the roles of abnormal myogenic responsiveness and dyslipidemia. *Circulation*. 2002 Dec 10;106(24):3037-43.

98. Furuse J, Maru Y, Mera K, Sumi H, Yoshino M, Yokoyama Y, et al. Visualization of blood flow in hepatic vessels and hepatocellular carcinoma using B-flow sonography. *J Clin Ultrasound*. 2001 Jan;29(1):1-6.

99. Naruo K, Miyamoto Y, Irie T, Sakuma T, Takeuchi H, Sirakawa T, et al. [Clinical usefulness of B-flow imaging in the diagnosis of superficial soft tissue tumors]. *Nihon Igaku Hoshasen Gakkai Zasshi*. 2005 Oct;65(4):393-8.

100. Weskott HP. [B-flow--a new method for detecting blood flow]. *Ultraschall Med*. 2000 Apr;21(2):59-65.

101. Ascher E, Hingorani A, Markevich N, Costa T, Kallakuri S, Khanimoy Y. Lower extremity revascularization without preoperative contrast arteriography: experience with duplex ultrasound arterial mapping in 485 cases. *Ann Vasc Surg*. 2002 Jan;16(1):108-14.

102. Collins R, Burch J, Cranny G, Aguiar-Ib^o±ez R, Craig D, Wright K, et al. Duplex ultrasonography, magnetic resonance angiography, and computed tomography angiography for diagnosis and assessment of symptomatic, lower limb peripheral arterial disease: systematic review. *BMJ*. 2007 Jun 16;334(7606):1257.

103. Cossman DV, Ellison JE, Wagner WH, Carroll RM, Treiman RL, Foran RF, et al. Comparison of contrast arteriography to arterial mapping with color-flow duplex imaging in the lower extremities. *J Vasc Surg*. 1989 Nov;10(5):522-8; discussion 8-9.

104. Collins R, Cranny G, Burch J, Aguiar-Ib^o±ez R, Craig D, Wright K, et al. A systematic review of duplex ultrasound, magnetic resonance angiography and computed tomography angiography for the diagnosis and assessment of symptomatic, lower limb peripheral arterial disease. *Health Technol Assess*. 2007 May;11(20):iii-iv, xi-xiii, 1-184.

105. Aboyans V, Ricco JB, Bartelink MEL, Bj^orck M, Brodmann M, Cohnert T, et al. Editor's Choice - 2017 ESC Guidelines on the Diagnosis and Treatment of Peripheral Arterial Diseases, in collaboration with the European Society for Vascular Surgery (ESVS). *Eur J Vasc Endovasc Surg*. 2018 Mar;55(3):305-68.

106. Akai T, Yamamoto K, Okamoto H, Shigematsu K, Otsu H, Watanabe T, et al. Usefulness of the Bollinger scoring method in evaluating peripheral artery angiography with 64-low computed tomography in patients with peripheral arterial disease. *Int Angiol*. 2014 Oct;33(5):426-33.

107. Bradbury AW, Adam DJ, Bell J, Forbes JF, Fowkes FG, Gillespie I, et al. Bypass versus Angioplasty in Severe Ischaemia of the Leg (BASIL) trial: An intention-to-treat analysis of amputation-free and overall survival in patients randomized to a bypass surgery-first or a balloon angioplasty-first revascularization strategy. *J Vasc Surg*. 2010 May;51(5 Suppl):5S-17S.

108. Zielinski LP, Chowdhury MM, Carter M, Worsfold BP, Coughlin PA. Variability in Atherosclerotic Disease Progression within the Infrainguinal Arterial Circulation is Dependent on Both Patient and Anatomical Factors. *Ann Vasc Surg*. 2017 Oct;44:289-98.

109. Gerhard-Herman M, Gardin JM, Jaff M, Mohler E, Roman M, Naqvi TZ. Guidelines for noninvasive vascular laboratory testing: a report from the American Society of Echocardiography and the Society for Vascular Medicine and Biology. *Vasc Med*. 2006 Nov;11(3):183-200.

110. Benitez E, Sumpio BJ, Chin J, Sumpio BE. Contemporary assessment of foot perfusion in patients with critical limb ischemia. *Semin Vasc Surg*. 2014 Mar;27(1):3-15.

111. Hanafee W, Stout P. Subtraction technic. *Radiology*. 1962 Oct;79:658-61.

112. Jeans WD. The development and use of digital subtraction angiography. *Br J Radiol*. 1990 Mar;63(747):161-8.

113. Palena LM, Diaz-Sandoval LJ, Candeo A, Brigato C, Sultato E, Manzi M. Automated Carbon

- Dioxide Angiography for the Evaluation and Endovascular Treatment of Diabetic Patients With Critical Limb Ischemia. *J Endovasc Ther.* 2016 Feb;23(1):40-8.
114. Dorweiler B, Neufang A, Kreitner KF, Schmiedt W, Oelert H. Magnetic resonance angiography unmasks reliable target vessels for pedal bypass grafting in patients with diabetes mellitus. *J Vasc Surg.* 2002 Apr;35(4):766-72.
115. Bartels LW, Smits HF, Bakker CJ, Viergever MA. MR imaging of vascular stents: effects of susceptibility, flow, and radiofrequency eddy currents. *J Vasc Interv Radiol.* 2001 Mar;12(3):365-71.
116. Koelemay MJ, Lijmer JG, Stoker J, Legemate DA, Bossuyt PM. Magnetic resonance angiography for the evaluation of lower extremity arterial disease: a meta-analysis. *JAMA.* 2001 Mar 14;285(10):1338-45.
117. Lapeyre M, Kobeiter H, Desgranges P, Rahmouni A, Becquemin JP, Luciani A. Assessment of critical limb ischemia in patients with diabetes: comparison of MR angiography and digital subtraction angiography. *AJR Am J Roentgenol.* 2005 Dec;185(6):1641-50.
118. Loewe C, Schoder M, Rand T, Hoffmann U, Sailer J, Kos T, et al. Peripheral vascular occlusive disease: evaluation with contrast-enhanced moving-bed MR angiography versus digital subtraction angiography in 106 patients. *AJR Am J Roentgenol.* 2002 Oct;179(4):1013-21.
119. Morasch MD, Collins J, Pereles FS, Carr JC, Eskandari MK, Pearce WH, et al. Lower extremity stepping-table magnetic resonance angiography with multilevel contrast timing and segmented contrast infusion. *J Vasc Surg.* 2003 Jan;37(1):62-71.
120. Owen RS, Carpenter JP, Baum RA, Perloff LJ, Cope C. Magnetic resonance imaging of angiographically occult runoff vessels in peripheral arterial occlusive disease. *N Engl J Med.* 1992 Jun 11;326(24):1577-81.
121. Prince MR, Chabra SG, Watts R, Chen CZ, Winchester PA, Khilnani NM, et al. Contrast material travel times in patients undergoing peripheral MR angiography. *Radiology.* 2002 Jul;224(1):55-61.
122. Wang Y, Truong TN, Yen C, Bilecen D, Watts R, Trost DW, et al. Quantitative evaluation of susceptibility and shielding effects of nitinol, platinum, cobalt-alloy, and stainless steel stents. *Magn Reson Med.* 2003 May;49(5):972-6.
123. Wang Y, Winchester PA, Khilnani NM, Lee HM, Watts R, Trost DW, et al. Contrast-enhanced peripheral MR angiography from the abdominal aorta to the pedal arteries: combined dynamic two-dimensional and bolus-chase three-dimensional acquisitions. *Invest Radiol.* 2001 Mar;36(3):170-7.
124. Bridges MD, St Amant BS, McNeil RB, Cernigliaro JG, Dwyer JP, Fitzpatrick PM. High-dose gadodiamide for catheter angiography and CT in patients with varying degrees of renal insufficiency: Prevalence of subsequent nephrogenic systemic fibrosis and decline in renal function. *AJR Am J Roentgenol.* 2009 Jun;192(6):1538-43.
125. Guerrero A, Montes R, Muñoz-Terol J, Gil-Peralta A, Toro J, Naranjo M, et al. Peripheral arterial disease in patients with stages IV and V chronic renal failure. *Nephrol Dial Transplant.* 2006 Dec;21(12):3525-31.
126. Hodnett PA, Ward EV, Davarpanah AH, Scanlon TG, Collins JD, Glielmi CB, et al. Peripheral arterial disease in a symptomatic diabetic population: prospective comparison of rapid unenhanced MR angiography (MRA) with contrast-enhanced MRA. *AJR Am J Roentgenol.* 2011 Dec;197(6):1466-73.
127. Lim RP, Hecht EM, Xu J, Babb JS, Oesingmann N, Wong S, et al. 3D nongadolinium-enhanced ECG-gated MRA of the distal lower extremities: preliminary clinical experience. *J Magn Reson Imaging.* 2008 Jul;28(1):181-9.
128. Varga-Szemes A, Wichmann JL, Schoepf UJ, Suranyi P, De Cecco CN, Muscogiuri G, et al. Accuracy of Noncontrast Quiescent-Interval Single-Shot Lower Extremity MR Angiography Versus CT- \uparrow Angiography for Diagnosis of Peripheral Artery Disease: Comparison With Digital Subtraction Angiography. *JACC Cardiovasc Imaging.* 2017 Oct;10(10 Pt A):1116-24.
129. Lowry D, Saeed M, Narendran P, Tiwari A. A Review of Distribution of Atherosclerosis in the

- Lower Limb Arteries of Patients With Diabetes Mellitus and Peripheral Vascular Disease. *Vasc Endovascular Surg.* 2018 Oct;52(7):535-42.
130. Bishop PD, Feiten LE, Ouriel K, Nassoioy SP, Pavkov ML, Clair DG, et al. Arterial calcification increases in distal arteries in patients with peripheral arterial disease. *Ann Vasc Surg.* 2008 Nov;22(6):799-805.
131. Kau T, Eicher W, Reiterer C, Niedermayer M, Rabitsch E, Senft B, et al. Dual-energy CT angiography in peripheral arterial occlusive disease-accuracy of maximum intensity projections in clinical routine and subgroup analysis. *Eur Radiol.* 2011 Aug;21(8):1677-86.
132. Meyer BC, Werncke T, Foert E, Kruschewski M, Hopfenmüller W, Ribbe C, et al. Do the cardiovascular risk profile and the degree of arterial wall calcification influence the performance of MDCT angiography of lower extremity arteries? *Eur Radiol.* 2010 Feb;20(2):497-505.
133. Nguyen GK, Hwang BH, Zhang Y, Monahan JF, Davis GB, Lee YS, et al. Novel biomarkers of arterial and venous ischemia in microvascular flaps. *PLoS One.* 2013;8(8):e71628.
134. Swanberg J, Nyman R, Magnusson A, Wanhainen A. Selective intra-arterial dual-energy CT angiography (s-CTA) in lower extremity arterial occlusive disease. *Eur J Vasc Endovasc Surg.* 2014 Sep;48(3):325-9.
135. Tanaka R, Yoshioka K, Takagi H, Schuijf JD, Arakita K. Novel developments in non-invasive imaging of peripheral arterial disease with CT: experience with state-of-the-art, ultra-high-resolution CT and subtraction imaging. *Clin Radiol.* 2019 Jan;74(1):51-8.
136. Yunaga H, Ohta Y, Kaetsu Y, Kitao S, Watanabe T, Furuse Y, et al. Diagnostic performance of calcification-suppressed coronary CT angiography using rapid kilovolt-switching dual-energy CT. *Eur Radiol.* 2017 Jul;27(7):2794-801.
137. Zimmerman SL, Fishman EK. Upper and lower limb imaging. In: Carrascosa PM, Cury RC, Garcia MJ, editors. *Dual-energy CT in cardiovascular imaging.* Cham: Springer International Publishing; 2015. p. 129-48.
138. Buls N, de Brucker Y, Aerden D, Devos H, Van Gompel G, Boonen PT, et al. Improving the diagnosis of peripheral arterial disease in below-the-knee arteries by adding time-resolved CT scan series to conventional run-off CT angiography. First experience with a 256-slice CT scanner. *Eur J Radiol.* 2019 Jan;110:136-41.
139. Conte MS, Pomposelli FB, Clair DG, Geraghty PJ, McKinsey JF, Mills JL, et al. Society for Vascular Surgery practice guidelines for atherosclerotic occlusive disease of the lower extremities: management of asymptomatic disease and claudication. *J Vasc Surg.* 2015 Mar;61(3 Suppl):2S-41S.
140. Gerhard-Herman MD, Gornik HL, Barrett C, Barshes NR, Corriere MA, Drachman DE, et al. 2016 AHA/ACC Guideline on the Management of Patients With Lower Extremity Peripheral Artery Disease: Executive Summary: A Report of the American College of Cardiology/American Heart Association Task Force on Clinical Practice Guidelines. *J Am Coll Cardiol.* 2017 Mar 21;69(11):1465-508.
141. Hirsch AT, Haskal ZJ, Hertzner NR, Bakal CW, Creager MA, Halperin JL, et al. ACC/AHA 2005 Practice Guidelines for the management of patients with peripheral arterial disease (lower extremity, renal, mesenteric, and abdominal aortic): a collaborative report from the American Association for Vascular Surgery/Society for Vascular Surgery, Society for Cardiovascular Angiography and Interventions, Society for Vascular Medicine and Biology, Society of Interventional Radiology, and the ACC/AHA Task Force on Practice Guidelines (Writing Committee to Develop Guidelines for the Management of Patients With Peripheral Arterial Disease): endorsed by the American Association of Cardiovascular and Pulmonary Rehabilitation; National Heart, Lung, and Blood Institute; Society for Vascular Nursing; TransAtlantic Inter-Society Consensus; and Vascular Disease Foundation. *Circulation.* 2006 Mar 21;113(11):e463-654.
142. Tenders M, Aboyans V, Bartelink ML, Baumgartner I, Clement D, Collet JP, et al. ESC Guidelines on the diagnosis and treatment of peripheral artery diseases: Document covering atherosclerotic disease of extracranial carotid and vertebral, mesenteric, renal, upper and lower extremity arteries: the Task

Force on the Diagnosis and Treatment of Peripheral Artery Diseases of the European Society of Cardiology (ESC). *Eur Heart J*. 2011 Nov;32(22):2851-906.

143. Rekha G, Prema GS, Padmini O. Somatosensory evoked potentials in diabetes mellitus type-2. *Journal of Evidence Based Medicine and Healthcare*. 2015;43(2):7594-601.

144. Lyons TE, Rosenblum BI, Veves A. Foot Pressure Abnormalities in the Diabetic Foot. In: Veves A, Giurini JM, Legerfo FW, editors. *The Diabetic Foot Contemporary Diabetes*: Humana Press; 2006.

145. Sutkowska E, Sutkowski K, Sokołowski M, Franek E, Dragan S, Sr. Distribution of the Highest Plantar Pressure Regions in Patients with Diabetes and Its Association with Peripheral Neuropathy, Gender, Age, and BMI: One Centre Study. *J Diabetes Res*. 2019;2019:7395769.

146. Razak AH, Zayegh A, Begg RK, Wahab Y. Foot plantar pressure measurement system: a review. *Sensors (Basel)*. 2012;12(7):9884-912.

147. Yudovsky D, Nouvong A, Schomacker K, Pilon L. Monitoring temporal development and healing of diabetic foot ulceration using hyperspectral imaging. *J Biophotonics*. 2011 Aug;4(7-8):565-76.

148. van Netten JJ, van Baal JG, Liu C, van der Heijden F, Bus SA. Infrared thermal imaging for automated detection of diabetic foot complications. *J Diabetes Sci Technol*. 2013 Sep 1;7(5):1122-9.

149. Todd C, Salvetti P, Naylor K, Albatat M. Towards Non-Invasive Extraction and Determination of Blood Glucose Levels. *Bioengineering (Basel)*. 2017 Sep 27;4(4).

150. Lahiri BB, Bagavathiappan S, Jayakumar T, Philip J. Medical applications of infrared thermography: A review. *Infrared Phys Technol*. 2012 Jul;55(4):221-35.

151. Liu C, van Netten JJ, van Baal JG, Bus SA, van der Heijden F. Automatic detection of diabetic foot complications with infrared thermography by asymmetric analysis. *J Biomed Opt*. 2015 Feb;20(2):26003.

152. Petrova NL, Whittam A, MacDonald A, Ainarkar S, Donaldson AN, Bevans J, et al. Reliability of a novel thermal imaging system for temperature assessment of healthy feet. *J Foot Ankle Res*. 2018;11:22.

153. Maldonado H, Bayareh R, Torres IA, Vera A, Leija L. Automatic Detection of Risk Zones in Diabetic Foot Soles by Processing Thermographic Images Taken in an Uncontrolled Environment. *Infrared Phys Technol*. 2020.

154. Eid MM, Yousef RN, Mohamed MA. A proposed automated system to classify diabetic foot from thermography. *Int J Sci Engin Res*. 2018;9(12):371-81.

155. Cruz-Vega I, Hernandez-Contreras D, Peregrina-Barreto H, Rangel-Magdaleno JJ, Ramirez-Cortes JM. Deep Learning Classification for Diabetic Foot Thermograms. *Sensors (Basel)*. 2020 Mar 22;20(6).

156. Vardasca R, Magalhaes C, Seixas A, Carvalho R, Mendes J, editors. Diabetic foot monitoring using dynamic thermography and AI classifiers. 3rd Quantitative InfraRed Thermography Asia Conference (QIRT Asia 2019); 2019 July; Tokyo, Japan.

157. Adam M, Ng EYK, Oh SL, Heng ML, Hagiwara Y, Tan JH, et al. Automated detection of diabetic foot with and without neuropathy using double density-dual tree-complex wavelet transform on foot thermograms. *Infrared Phys Technol*. 2018 August;92:270-9.

158. van Doremalen RFM, van Netten JJ, van Baal JG, Vollenbroek-Hutten MMR, van der Heijden F. Infrared 3D Thermography for Inflammation Detection in Diabetic Foot Disease: A Proof of Concept. *J Diabetes Sci Technol*. 2020 Jan;14(1):46-54.

159. Astasio-Picado A, Martinez EE, Nova AM, Rodriguez RS, Gomez-Martin B. Thermal map of the diabetic foot using infrared thermography. *Infrared Phys Technol*. 2018;93:59-62.

160. Yavuz M, Ersen A, Hartos J, Lavery LA, Wukich DK, Hirschman GB, et al. Temperature as a Causative Factor in Diabetic Foot Ulcers: A Call to Revisit Ulceration Pathomechanics. *J Am Podiatr Med Assoc*. 2019 Sep;109(5):345-50.

161. Fraiwan L, Ninan J, Al-Khodari M. Mobile Application for Ulcer Detection. *Open Biomed Eng J*. 2018;12:16-26.

162. Neves EB, Almeida A, Rosa C, Alves JV, editors. Anthropometric Profile and Diabetic Foot Risk: A Cross-Sectional Study Using Thermography. 37th Annual International Conference of the IEEE

Engineering in Medicine and Biology Society (EMBC); 2015.

163. Keenan E, Gethin G, Flynn L, Watterson D, O'Connor GM. Enhanced thermal imaging of wound tissue for better clinical decision making. *Physiol Meas*. 2017 Jun;38(6):1104-15.

164. Khaodhiar L, Dinh T, Schomacker KT, Panasyuk SV, Freeman JE, Lew R, et al. The use of medical hyperspectral technology to evaluate microcirculatory changes in diabetic foot ulcers and to predict clinical outcomes. *Diabetes Care*. 2007 Apr;30(4):903-10.

165. Yang Q, Sun S, Jeffcoate WJ, Clark DJ, Musgrove A, Game FL, et al. Investigation of the Performance of Hyperspectral Imaging by Principal Component Analysis in the Prediction of Healing of Diabetic Foot Ulcers. *J Imaging*. 2018;4(12):144.

166. Greenman RL, Panasyuk S, Wang X, Lyons TE, Dinh T, Longoria L, et al. Early changes in the skin microcirculation and muscle metabolism of the diabetic foot. *Lancet*. 2005 Nov 12;366(9498):1711-7.

167. Jeffcoate WJ, Clark DJ, Savic N, Rodmell PI, Hinchliffe RJ, Musgrove A, et al. Use of HSI to measure oxygen saturation in the lower limb and its correlation with healing of foot ulcers in diabetes. *Diabet Med*. 2015 Jun;32(6):798-802.

168. Nouvong A, Hoogwerf B, Mohler E, Davis B, Tajaddini A, Medenilla E. Evaluation of diabetic foot ulcer healing with hyperspectral imaging of oxyhemoglobin and deoxyhemoglobin. *Diabetes Care*. 2009 Nov;32(11):2056-61.

169. Kottmann J, Rey JM, Luginbuhl J, Reichmann E, Sigrist MW. Glucose sensing in human epidermis using mid-infrared photoacoustic detection. *Biomed Opt Express*. 2012 Apr 1;3(4):667-80.

170. Goyal M, Reeves ND, Davison AK, Rajbhandari S, Spragg J. DFUNet: Convolutional Neural Networks for Diabetic Foot Ulcer Classification. *IEEE Transactions on Emerging Topics in Computational Intelligence*. 2018:1-12.

171. Raizada A, Johri V, Ramnath T, Chowdhary D, Garg R. A cross-sectional study on the palmar dermatoglyphics in relation to carcinoma breast patients. *J Clin Diagn Res*. 2013;7(4):609-612.
doi:10.7860/JCDR/2013/4689.2864